

Polygenicity and epistasis underlie fitness-proximal traits in the *Caenorhabditis elegans* multiparental experimental evolution (CeMEE) panel

Luke M. Noble^{*,1}, Ivo Chelo[†], Thiago Guzella[§], Bruno Afonso^{§,†}, David D. Riccardi^{*}, Patrick Ammerman^{*}, Adel Dayarian^{**}, Sara Carvalho[†], Anna Crist[§], Ania Pino-Querido[†], Boris Shraiman^{**,†}, Matthew V. Rockman^{*,1} and Henrique Teotónio^{§,1}

^{*}Center for Genomics and Systems Biology, Department of Biology, New York University, New York, NY, 10003, USA, [†]Instituto Gulbenkian de Ciência, Oeiras, Portugal, [§]Institut de Biologie, École Normale Supérieure, CNRS UMR 8197, INSERM U1024, F-75005 Paris, France, ^{**}Kavli Institute for Theoretical Physics and, [†]Department of Physics, University of California, Santa Barbara, CA, 93106, USA

ABSTRACT Understanding the genetic basis of complex traits remains a major challenge in biology. Polygenicity, phenotypic plasticity and epistasis contribute to phenotypic variance in ways that are rarely clear. This uncertainty is problematic for estimating heritability, for predicting individual phenotypes from genomic data, and for parameterizing models of phenotypic evolution. Here we report a recombinant inbred line (RIL) quantitative trait locus (QTL) mapping panel for the hermaphroditic nematode *Caenorhabditis elegans*, the *C. elegans* multiparental experimental evolution (CeMEE) panel. The CeMEE panel, comprising 507 RILs, was created by hybridization of 16 wild isolates, experimental evolution at moderate population sizes and predominant outcrossing for 140-190 generations, and inbreeding by selfing for 13-16 generations. The panel contains 22% of single nucleotide polymorphisms known to segregate in natural populations, and complements existing mapping resources for *C. elegans* by providing high nucleotide diversity across >95% of the genome. We apply it to study the genetic basis of two fitness components, fertility and hermaphrodite body size at time of reproduction, with high broad sense heritability in the CeMEE. While simulations show we should detect common alleles with additive effects as small as 5%, at gene-level resolution, the genetic architectures of these traits does not feature such alleles. We instead find that a significant fraction of trait variance, particularly for fertility, can be explained by sign epistasis with weak main effects. In congruence, phenotype prediction, while generally poor ($r^2 < 10\%$), requires modeling epistasis for optimal accuracy, with most variance attributed to the highly recombinant, rapidly evolving chromosome arms.

KEYWORDS genetic architecture; polygenicity; epistasis; experimental evolution; body size; fertility; selfing; GWAS; heritability; quantitative trait; complex trait; QTL; MPP

Introduction

Most measurable features of organisms vary among individuals. Outlining the genetic dimension of this variation, and how this varies across populations and traits, has important implications for the application of genomic data to predict disease risk and agricultural production, for estimation of heritability, and for understanding evolution (Lynch and Walsh 1998; Barton and Keightley 2002). Complex traits are defined by being multifactorial. They tend to be influenced by many genes and to be plastic in the presence of environmental variation, and the manner in which phenotypic variation emerges from the combined effects

of causal alleles is rarely clear. Although phenotype prediction and some aspects of evolution can often be well approximated by considering additive effects alone, non-additive interactions between alleles at different loci (with marginal additive effects) may explain a large fraction of trait variation yet remain undetected due to low statistical power (Phillips 2008). Adding further complication, one cannot usually assume that genetic and environmental effects are homogeneous or independent of one another (Barton and Turelli 1991; Félix and Barkoulas 2015), nor that the genetic markers used for mapping quantitative trait loci (QTL) are faithfully and uniformly associated with causal alleles (Yang *et al.* 2010; Speed *et al.* 2012).

Human height, for example, is the canonical quantitative trait, an easily measured, stable attribute with high heritability (around 80%) when measured in families Fisher (1930); Galton (1886); Visscher *et al.* (2010). Hundreds of common QTL (minor allele frequency, MAF>5%) of small effect have been detected by genome-wide association studies (GWAS) over the last two decades, explaining in sum only a small fraction (around 20%) of heritability (Wood *et al.* 2014). A recent study with more than 7×10^5 people showed that close to one hundred uncommon QTLs (0.1%<MAF<5%) of more moderate effects explain a mere extra 5% of heritability (Marouli *et al.* 2017). It has taken methods of genomic selection in animal breeding, and dense genetic marker information (Meuwissen *et al.* 2001; Meuwissen and Goddard 2010), to show that common QTL of very small effect can potentially explain a large fraction of the variability in human height and common diseases (Yang *et al.* 2010; Speed *et al.* 2016). Thus, in perhaps many cases, the so-called problem of the “missing heritability” may be synonymous with high polygenicity (Hill *et al.* 2008; Manolio *et al.* 2009). The contribution of statistical epistasis to variation in human height is likely to be modest (Visscher *et al.* 2010), although the generality of this for size-related traits in other organisms is not known. Molecular genetics and biochemistry suggest functional non-additivity is ubiquitous within individuals, and significant effects on trait variation have been shown in many cases (e.g., MUKAI (1967); Whitlock and Bourguet (2000); Bonhoeffer *et al.* (2004); Carlborg *et al.* (2006); de Visser *et al.* (2009); Zwarts *et al.* (2011); Shao *et al.* (2008); Gaertner *et al.* (2012); Barkoulas *et al.* (2013); Weinreich *et al.* (2013); Huang *et al.* (2014); Vanhaeren *et al.* (2014); Bloom *et al.* (2015); Monnahan and Kelly (2015b,a); Paaby *et al.* (2015); Tyler *et al.* (2016); Schoustra *et al.* (2016); Forsberg *et al.* (2017); Chirgwin *et al.* (2016), but the importance of epistasis in shaping fitness landscapes and in generating the additive genetic variance on which selection can act is still debated (Cheverud and Routman 1995; Wolf *et al.* 2000; Phillips 2008; Hansen 2013; Mackay *et al.* 2014)).

Alongside GWAS, inbred line crosses in model systems continue to be instrumental for our understanding of the genetics of complex traits, given the opportunity for control of confounding environmental covariates and accurate measurement of breeding values. Crosses among multiple parental strains in particular – such as those now available for mice (Churchill *et al.* 2004), *Drosophila* (Macdonald and Long 2007), maize (McMullen *et al.* 2009; Buckler *et al.* 2009), wheat (Huang *et al.* 2012; Mackay *et al.* 2014; Thepot *et al.* 2015), rice (Bandillo *et al.* 2013), tomato (Pascoal *et al.* 2015) and *Arabidopsis* (Kover *et al.* 2009), among others – have been developed to better sample natural genetic variation. Greater variation also allows the effects of multiallelic loci to be studied and, subject to effective recombination, improved QTL resolution. If large populations and random mating are imposed for long periods, gains in resolution can be dramatic (Valdar *et al.* 2006; Rockman and Kruglyak 2008), although this comes at the expense of increased opportunity for selection to purge diversity (e.g., Baldwin-Brown *et al.* (2014); Rockman and Kruglyak (2009)).

Better known as a model for functional biology (Corsi *et al.* 2015), the nematode *Caenorhabditis elegans* has also contributed to our understanding of complex traits and their evolution. *C. elegans* shows extensive variation in complex traits (Gems and Riddle 2000; Knight *et al.* 2001; Barrière and Félix 2005; Gutteling *et al.* 2007; Gray and Cutter 2014; Diaz and Viney 2014; Teotónio *et al.* 2017) and sex-determination and breeding mode (selfing

and outcrossing) can be genetically manipulated at will. QTL for traits such as embryonic lethality (Rockman and Kruglyak 2009), pesticide resistance (Ghosh *et al.* 2012) and telomere length (Cook *et al.* 2016) have been found by association studies in an ever expanding panel of inbred wild isolates, the *C. elegans* natural diversity resource (CeNDR; <https://elegansvariation.org/>, Cook *et al.* (2017)). QTL for a range of complex traits have also been found using collections of recombinant inbred lines (RILs) (Rockman and Kruglyak 2009) and introgression lines (ILs) (Doroszuk *et al.* 2009) derived from crossing the laboratory domesticated N2 strain (Sterken *et al.* 2015) and the divergent Hawaiian wild isolate CB4856 (e.g., Andersen *et al.* (2014, 2015)), or by two-parent crossing of non-domesticated strains (e.g., Duveau and Félix (2012); Noble *et al.* (2015)). GWAS and two-parent crosses have given insights into how natural selection has shaped phenotypic variation in *C. elegans* and related nematodes. For example, an N2/CB4856 RIL panel has been used to argue that selection on linked sites largely explains the distribution of QTL effects for mRNA abundance (Rockman *et al.* 2010). Lastly, *C. elegans* is also one of the main models for experimental evolution (Gray and Cutter 2014; Teotónio *et al.* 2017). Mutation accumulation line panels in particular have long been used to estimate mutational heritability (Estes and Lynch 2003; Estes 2005; Baer *et al.* 2005; Baer 2008; Phillips *et al.* 2009; Halligan and Keightley 2009) and to argue that standing levels of genetic variation in natural populations for complex traits can be explained by a mutation-selection balance (Etienne *et al.* 2015; Farhadifar *et al.* 2016). As yet, the QTL mapping resolution of existing *C. elegans* RIL panels has been coarse, and there is no panel derived from crosses of multiple wild parental strains.

A prominent characteristic of *C. elegans* is its mixed androdioecious reproductive system, with hermaphrodites capable of either selfing, from a cache of sperm produced late in larval development (Hirsh *et al.* 1976), or outcrossing with males (Maupas 1900). Sex determination is chromosomal, with hermaphrodites XX, and XO males maintained through crosses and rare X-chromosome non-disjunction during hermaphrodite gametogenesis (Nigon 1949). Because males are typically absent from selfed broods but are half the progeny of a cross, twice the male frequency in a population is the expected outcrossing rate (Stewart and Phillips 2002; Cutter 2004). Natural populations have low genetic diversity and very high linkage disequilibrium (LD), with generally weak global population structure and high local diversity among typically homozygous individuals at the patch scale (Barrière and Félix 2005, 2007; Cutter *et al.* 2009). Average single nucleotide polymorphism (SNP) diversity is on the order of 0.3% (Cutter 2006) though highly variable across the genome, reaching 16% or more in some hypervariable regions (Thompson *et al.* 2015). Low diversity and high LD is due to the predominance of inbreeding by selfing, which reduces the effective recombination rate and elevates susceptibility to linked selection (Rockman *et al.* 2010; Andersen *et al.* 2012). Crosses between wild isolates have revealed outbreeding depression (Dolgin *et al.* 2007; Chelo *et al.* 2014), which may be in part due to the disruption of epistatic allelic interactions. Evidence supporting this prediction in *C. elegans* is, to date, scarce: one study has shown that recombination between several QTL “complexes” leads to dysregulation of thermal preferences (Gaertner *et al.* 2012).

Although selfing is the most common reproductive mode in natural *C. elegans* populations, males, though rare, are variably proficient in mating with hermaphrodites (Teotónio *et al.* 2006;

Murray *et al.* 2011). Perhaps as a consequence of low but significant outcrossing (and also a metapopulation demographic structure) several loci have been found to be under some form of balancing selection (e.g., Ghosh *et al.* (2012); Greene *et al.* (2016)). Moreover, evolution experiments involving crosses among multiple strains have shown that high outcrossing rates can persist as long as there is heritable variation for male traits (Anderson *et al.* 2010; Teotónio *et al.* 2012; Masri *et al.* 2013). In our evolution experiments in particular (Teotónio *et al.* 2012), moderate population sizes and high outcrossing rates facilitated the loss of genetic diversity by (partial) selective sweeps, with excess heterozygosity maintained by epistatic selection on overdominant loci (e.g., Chelo and Teotónio (2013); Chelo *et al.* (2014)).

This foundation suggests study of *C. elegans* may be fruitful for our understanding of the contribution of within- and between-locus interactions to complex traits and their evolution. Here we present a panel of 507 genome sequenced RILs obtained by intercrossing 16 wild isolates, culturing at high outcrossing rates in populations of $\approx 10^4$ for 140-190 generations of experimental evolution, followed by inbreeding by selfing for 13-16 generations. The *C. elegans* Multiparental Experimental Evolution (CeMEE) RIL panel complements existing *C. elegans* mapping resources by providing fine mapping resolution and high nucleotide diversity. Using simulations, we show that the CeMEE panel can give gene-level resolution for common QTL with effects as low as 5%. In subsets of the CeMEE, we investigate the genetic basis of two fitness components, fertility and hermaphrodite body size at the time of reproduction, by variance decomposition under additive and additive-by-additive epistatic models, and by genome-wide 1- and 2-dimensional association testing. We find that the genetic basis of both traits, particularly fertility, is highly polygenic, with a significant role for epistasis.

Materials and Methods

CeMEE derivation

The panel was derived in 3 stages (Figure 1). First, 16 wild isolates (AB1, CB4507, CB4858, CB4855, CB4852, CB4586, MY1, MY16, JU319, JU345, JU400, N2 (ancestral), PB306, PX174, PX179, RC301; obtained from the Caenorhaditis Genetics Center) were inbred by selfing for 10 generations to ensure homozygosity, then intercrossed to funnel variation into a single multiparental hybrid population, as described in Teotónio *et al.* (2012). Each of the four funnel phases comprised multiple pairwise, reciprocal crosses at moderate population sizes (see Figure S1 of Teotónio *et al.* (2012) for full details of replication and population sizes).

Second, the multiparental hybrid population was evolved for 140 discrete generations at population sizes of $N \approx 10^4$ (outcrossing rate ≈ 0.5 , $N_e \approx 10^3$), to obtain the A140 population, as reported in (Teotónio *et al.* 2012; Chelo and Teotónio 2013; Chelo *et al.* 2013). Sex-determination mutations were then mass introgressed into the A140, while maintaining genetic diversity, to generate monoecious (obligately selfing hermaphrodites) and trioecious (partial selfing with males, females and hermaphrodites) populations, as detailed in Theologidis *et al.* (2014). Further replicated experimental evolution was carried out for 50 generations under two environmental regimes: (1) a Control regime (conditions as before), with the wild-type Androdioecious reproductive system (CA50 collectively, full designations can be found in Table S1); and (2) a Gradual exposure to an increasing gradient of NaCl, from 25mM (standard NGM-lite medium, US Biological) to 305mM until generation 35 and thereafter, vary-

ing reproductive system (GX50, where X is Androdioecious, Monoecious or Trioecious). Although trioecious populations started evolution with only 0.1% of hermaphrodites, by generation 50 they were abundant (50%; see Figure S7 in Theologidis *et al.* (2014)). Androdioecious populations maintained outcrossing rates of >0.4 until generation 35, soon after losing males to finish with an outcrossing rate of about 0.2 by generation 50 (Figure S5 in Theologidis *et al.* (2014)). The effects of reproductive system on the genetics and evolution of complex traits will be the subject of future work.

Finally, hermaphrodites were inbred by selfing to obtain recombinant inbred lines (RILs). Population samples ($> 10^3$ individuals) were thawed from -80C and maintained under standard laboratory conditions for two generations. At the third generation, single hermaphrodites were picked at the late third to early fourth (L3/L4) larval stage and placed in wells of 12-well culture plates, containing M9 medium (25mM NaCl) seeded with *E. coli*. Lines were propagated at 20C and 80% RH by transferring a single L3/L4 individual for 16 (A140 population) or 13 generations (4-7 days between transfers). At each passage, parental plates were kept at 4C to prevent growth until offspring production was verified, and in the case of failure a second transfer was attempted before declaring line extinction. Inbreeding was done in several blocks from 2012 to 2016, in two different labs. A total of 709 RILs were obtained and archived at -80C (File S2).

Sequencing and genotyping

DNA of the 16 founders, 666 RILs and the A140 population was prepared using the Qiagen Blood and Tissue kit soon after derivation or after thawing from frozen stocks and expansion to at least 10^4 L1 individuals. Founders were sequenced to $\geq 30X$ depth with 50 or 100bp paired-end reads (Illumina HiSeq 2000, New York University Center for Genomics and Systems Biology GenCore facility). Reads were mapped (BWA 0.7.8; Li and Durbin (2010)) to the WS220 *C. elegans* N2 reference genome and variants (SNPs and small indels) were called jointly (GATK 3.3-0 HaplotypeCaller; McKenna *et al.* (2010)), followed by base quality score recalibration (BQSR) using a subset of high scoring sites (29% of initial variants passing strict variant filtration: "MQ < 58.0 || DP < 20 || FS > 40.0 || SOR > 3.0 || ReadPosRankSum < -5.0 || QD < 20.0 || DP > mean \times 2"). Diallelic single nucleotide variants on the six nuclear chromosomes were intersected with calls from a joint three-sample call (GATK UnifiedGenotyper) on pooled founders, a subset of pooled RILs (SUP TABLE XX, SAME AS CEMEE LIST ANOTHER COLUMN), and 72X sequencing of the A140 population (approximately 1400x total), then filtered based on variant call metrics (MQ < 50.0 || DP < 10 || FS > 50.0 || SOR > 5.0 || ReadPosRankSum < -5.0 || QD < 6.0 || DP > mean \times 3) and on the number of heterozygous or missing founder calls (3,014 sites > 8 removed; these calls likely represent copy number differences between founders and the N2 reference), and requiring ≥ 1 homozygote (28,872 sites removed), giving an initial set of 404,536 SNP markers.

RILs were sequenced with 100bp paired-end reads (Nextera libraries, HiSeq 2000, NYU) or 150bp paired-end reads (HiSeq X Ten, BGI Tech Solutions Company, Hong Kong), to mean depth 7.2X (minimum 0.2X). Genotypes were imputed by Hidden Markov Model (HMM) considering the 16 founder states and mean base qualities of reads. Downsampled predictions for a subset of RILs sequenced to high (20-30X) depth gave imputation accuracy of approximately 99% at 0.2X and 99.9% at 0.5X (93% of lines).

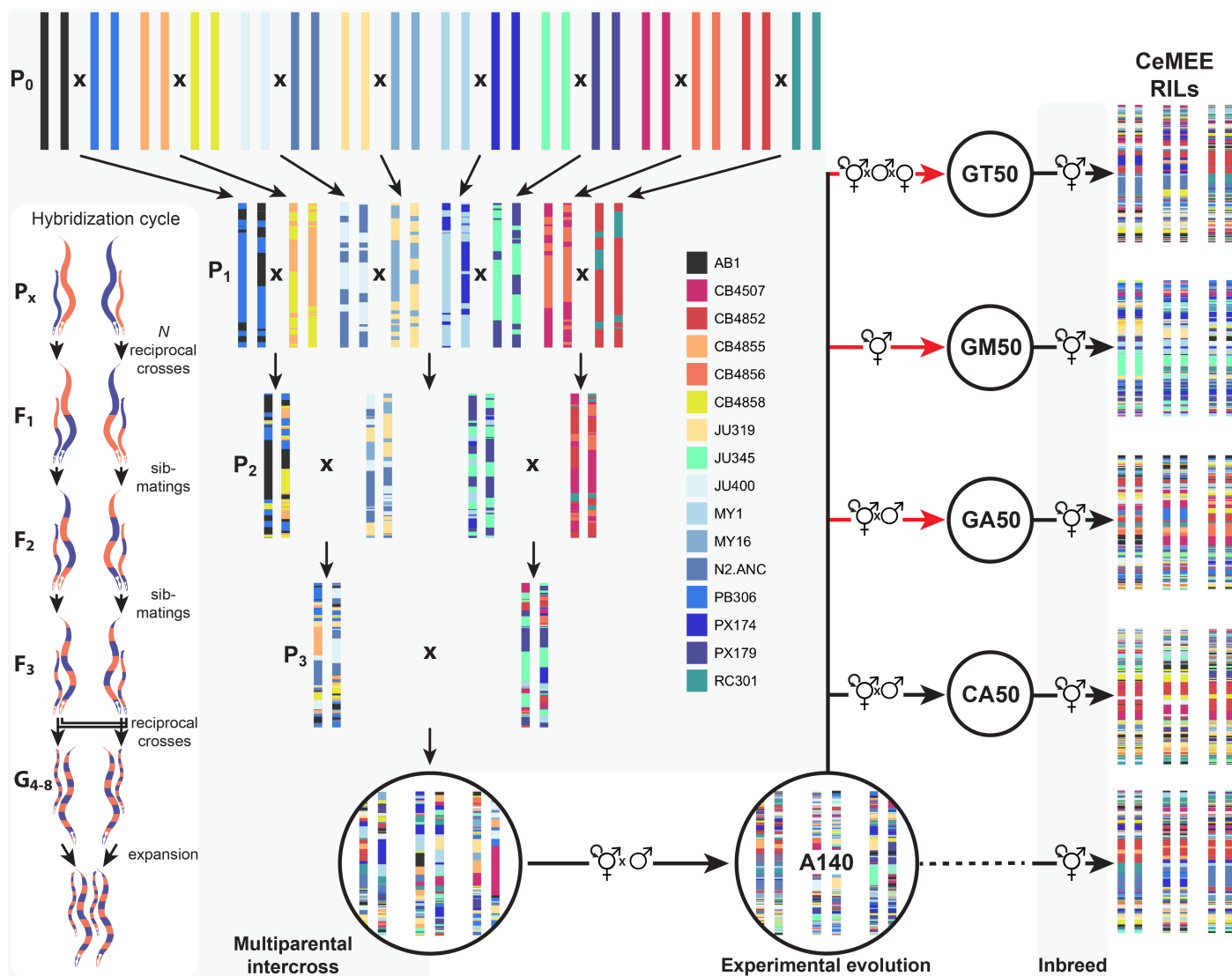


Figure 1 CeMEE derivation. The multiparental intercross funnel phase comprised four stages of pairwise crosses and progeny mixing, carried out in parallel at controlled population sizes. One hybridization cycle for a single founder cross is inset at left: in each cycle, multiple reciprocal crosses were initiated, increasing in replicate number and census size each filial generation. F_1 and F_2 progeny were first sib-mated, then reciprocal lines were merged by intercrossing the F_3 and expanding the pooled G_4 (for three to four generations) before commencing the next reduction cycle. The resulting multiparental hybrid population was archived by freezing, and samples were thawed and then maintained for 140 non-overlapping generations of mixed selfing and outcrossing under standard laboratory conditions to generate the A140 population. Hermaphrodites were then sampled from the A140 and selfed to generate the A140 RILs. Additionally, the outbred A140 population was evolved for a further 50 generations under the same conditions (control adapted lines; CA) or under adaptation to a salt gradient with varying sex ratios (GT, GM and GA lines; Theologidis *et al.* (2014)). See [Materials and Methods](#) for description of sub-panels, and [Teotónio *et al.* \(2012\)](#) for details of replicate numbers and population sizes for each funnel generation.

287 We assessed accuracy and appropriate variant filtering thresh- 347
288 olds by genotyping a set of 784 markers, uniformly distributed 348
289 across the six chromosomes according to the genetic distances 349
290 of Rockman and Kruglyak (2009), in 182 RILs with the iPlex 350
291 Sequenom MALDI-TOF platform (Bradić *et al.* 2011). Sequenom 351
292 data can be found in Table S2. We fitted a linear model with 352
293 counts of Illumina/Sequenom concordant cases as the response 353
294 variable, and all founder variant quality metrics together with 354
295 the number of missing or heterozygous calls in the founders, 355
296 the number of zero-coverage or potentially heterozygous sites 356
297 (with at least a single Illumina read for each genotype), variant 357
298 nucleotide identity, and reference nucleotide and dinucleotide 358
299 identity as explanatory variables. Concordance across sequenc- 359
300 ing platforms was 96.9% after (93.7% before) final filtering, and 360
301 we retained 388,201 diallelic SNPs as founder markers. We esti- 361
302 mated residual heterozygosity for 25 A140 lines sequenced 362
303 to >20X coverage (single sample calls using GATK 3.3-0 Hap- 363
304 lotypeCaller, variant filtration settings MQ < 50.0 || DP < 5 364
305 || MQRankSum < -12.5 || SOR > 6 || FS > 60.0 || Read- 365
306 PosRankSum < -8.0 || QD < 10.0 || DP > mean×3). Mean 366
307 heterozygosity at founder sites is 0.095% (standard deviation 367
308 0.042%, range 0.033-0.18%). 368

309 After removal of RILs sharing greater than the mean pairwise 369
310 identity + 5 standard deviations (84.8%, excluding monoecious 370
311 lines), we retained 178 A140 RILs, 118 CA50 RILs (from three 371
312 replicate populations), 127 GA50 RILs (three replicates), and 372
313 79 GT50 RILs (two replicates). The 98 GM50 RILs (two repli- 373
314 cates) are highly related on average and group together into a 374
315 small number of "isotypes". To prevent introduction of strong 375
316 structure, we discard all but five below the above panel-wide 376
317 pairwise identity threshold for the purposes of trait mapping. In 377
318 total, the CeMEE comprises 507 RILs from five sub-panels, with 378
319 352,583 of the founder markers segregating within it (File S3). 379

320 CeMEE genetic structure

321 **Differentiation from natural isolates and founders** We com- 384
322 pared similarity within and between the CeMEE RILs and 152 se- 385
323 quenced wild-isolates from the CeNDR panel (release 20160408). 386
324 The distributions for all pairwise genotype and haplotype (% 387
325 identity at 0.33cM scale in F_2 map distance) distances are plotted 388
326 in Figure 2, for 256,535 shared diallelic sites with no missing or 389
327 heterozygous calls. 390

328 Linkage disequilibrium (r^2) was computed for founders and 391
329 CeMEE RILs at the same set of sites (MAF >1/16, <5% ambigu- 392
330 ous imputed RIL genotypes and ≤ 1 heterozygous/missing 393
331 founder genotypes, then downsampled by 10 for computational 394
332 tractability), and plotted against genetic distances (obtained by 395
333 linear interpolation from the N2/CB4856 map, scaled to F_2 dis- 396
334 tances (Rockman and Kruglyak 2009). To assess the extent of 397
335 subtle, long-range linkage disequilibrium in the form of inter- 398
336 chromosomal structure, we compared r^2 among chromosomes 399
337 to a null distribution generated by permutation ($n=5000$). In 400
338 each permutation, filtered RIL genotypes (pruned of strong local 401
339 linkage $r^2 < 0.98$, no ambiguous calls) were randomly down- 402
340 sampled to equal size across chromosomes, split by chromosome, 403
341 then shuffled within each sub-panel before taking the mean cor- 404
342 relation across chromosomes (or omitting all single and pairwise 405
343 chromosome combinations) as test statistic. The effect of local 406
344 LD pruning is to reduce the weighting of large regions in strong 407
345 linkage in order to better assay weak interactions across the 408
346 remainder of the genome.

Reconstruction of ancestral haplotypes and genetic map ex- 347
348 **pansion** For each RIL, founder haplotypes were inferred with 349
the RABBIT HMM framework implemented in Mathematica 350
(Zheng *et al.* 2015), conditioning on the recombination frequen- 351
cies observed for the N2 x CB4856 RILs (scaled to F_2 map length) 352
(Rockman and Kruglyak 2009). Realized map expansion was 353
estimated by maximum likelihood for each chromosome, be- 354
fore full marginal reconstruction of each chromosome (explicitly 355
modeling recombination on the X and autosomes) using post- 356
rior decoding under the fully dependent homolog model (dep- 357
Model). Under this model, appropriate for fully inbred diploids, 358
chromosome homologs are assumed to have identical ancestral 359
origins (prior identity by descent probability $f = 1$), and the 360
recombination junction density (transition probability) is given 361
by the estimated map expansion (Ra) and genotyping error rates 362
(set to 5×10^{-5} for founders and 5×10^{-3} for RILs based on like- 363
lihood from a parameter sweep). Sites called as heterozygous 364
or missing in the founders, or unresolved to [0, 1] by the geno- 365
type imputation HMM were set to NA before reconstruction. 366
For reconstruction summaries, haplotype posterior probabilities 367
were filtered to >0.2, and haplotype lengths and breakpoints 368
were estimated from run lengths of marker assignments, taking 369
the single best haplotype (if present), maintaining haplotype 370
identity (if multiple assignments of equal probability), or the 371
first among equals otherwise. 372

To test reconstruction accuracy as a function of haplotype 373
length, we performed simulations of a pedigree varying only the 374
number of generations of random mating. Starting from a single 375
population representing all founders ($N=1000$, corresponding 376
to the expected N_e during experimental evolution), mating oc- 377
curred at random with equal contribution to the next generation. 378
Recombination between homologous chromosomes occurred at 379
a rate of 50cM, with full crossover interference, and the proba- 380
bility of meiotic crossover based on distances between marker 381
pairs obtained by linear interpolation of genetic positions (Rock- 382
man and Kruglyak 2009). For each chromosome, 10 simulations 383
were run sampling at 10, 25, 50, 100 and 150 generations, and 384
haplotype reconstruction was carried out as above. Maximum 385
likelihood estimates of realized map expansion for simulations 386
were used to calibrate a model for prediction of realized number 387
of generations in the RILs by chromosome. A 2nd degree poly- 388
nomial regression of Ra on the known number of generations was 389
significantly preferred over a linear fit by likelihood ratio test, 390
given significant underestimation as pedigree length increased 391
(approaching 10% at G_{150}). 392

Population stratification Population stratification was assessed 393
using (1) principal component decomposition, giving a uni- or 394
bivariate view of the importance of genetic structure associated 395
with CeMEE sub-panels, and (2) by supervised and unsuper- 396
vised discriminant analysis of principal components (DAPC; 397
Jombart *et al.* (2010)), giving an estimate of the fraction of princi- 398
pal component variance that best predicts sub-panel structure, 399
and an inference of population structure without regard to sub- 400
panel identities. In all cases decomposition was of scaled and 401
centered genotypes pruned of strong local LD ($r^2 < 0.98$), giving 402
all markers equal weight (and therefore more weight to low 403
frequency alleles). 404

Of the first 50 principal components, 10 are significantly as- 405
sociated with sub-panel identity (i.e., evolutionary history) by 406
ANOVA ($p < 0.05$ after Bonferroni correction), accounting for 407
just 3.9% of the variance in sum. Seven of the top 10 PCs are sig- 408
nificant, though others up to PC 38 are also associated, showing

that multiple sources of structure contribute to the major axes of variation. Fitting all pairs among the the top 50, two pairs (7 and 19, 13 and 14) are significant (again at a conservative Bonferroni adjusted threshold), resolving the GT50 RILs as most distinct.

For DAPC (R package *adegenet*, [Jombart \(2008\)](#)), we used 100 rounds of cross-validation to determine the number of principal components required to achieve optimal group assignment accuracy (the mean of per-group correct assignments). This value (40 PCs) was then used to infer groups by unsupervised *k*-means clustering (default settings of 10 starts, 10^5 iterations), with *k* selected on the Bayesian Information Criterion (BIC). Correspondence of inferred groups with known groups was tested by permutation. Given the contingency table *C*, where $C_{i,j}$ represents the number of lines known to be in sub-panel *i* and inferred to be in cluster *j*, the inferred values for each cluster (*js*) were shuffled among known groups (*is*) 10,000 times, with the sum of the variance among known groups taken as a summary statistic (high values reflecting significant overlap between inferred and known groups).

Phenotyping

Fertility In the experimental evolution scheme under which the CeMEE RILs were generated, a hermaphrodite's contribution to the next generation is the number of viable embryos that survive bleaching (laid, but unhatched, or held *in utero*) that subsequently hatch to L1 larvae 24h later. We treat this phenotype as fertility, and measured it for individual worms of 230 RILs. Each line was thawed and maintained for two generations under standard conditions ([Stiernagle 2006](#); [Teotónio et al. 2012](#); [Theologidis et al. 2014](#)), bleached to kill adults, then embryos were allowed to hatch and synchronize as L1 larvae. L1s were then moved to fresh plates seeded with *E. coli* and allowed to develop for 48 hours. Single L3-L4 staged hermaphrodite larvae were then placed into each well of 96-well plates using a micropipette and stereomicroscope. Plate wells contained NGM-lite + 100µg/ml ampicillin, previously inoculated with 1µl of an overnight culture of *E. coli* (HT115) and stored until usage at 4C (maximum 2 weeks before use). After transfer, plates were covered with Parafilm to prevent cross-contamination and incubated at 20C and 80% relative humidity (RH) until the following day. Embryos were extracted by adding bleach solution to wells (1M KOH, 5% NaClO 1:1 v/v in M9 buffer) for 5 minutes, then 200µl of the extract was removed and rinsed 3 times in M9 buffer by centrifugation. The M9 suspension (200µl) was then transferred to another 96-well plate containing 120µl of M9 per well. Plates were incubated overnight (as above), then centrifuged for 1 min at 1800rpm to sediment any swimming larvae before imaging at 4 pixel/µm² with a Nikon Eclipse TE2000-S inverted microscope. [ImageJ](#) was then used to manually count the number of live (moving) L1s in each well. During assay setup and image analysis wells were censored where: bacteria were absent; hermaphrodites were absent or dead at the time of bleach; males had been inadvertently picked; more than 1 adult was present; or hermaphrodites had not been killed upon bleaching. Except for density between the L4 stage until reproduction, all assay conditions were the same as those used during experimental evolution. Fertility measurements do not include potential survival differences between the L1 stage until reproduction, but we nonetheless take it as a surrogate for fitness ([Chelo et al. 2013](#)).

Two independent plates within a single thaw were set-up for most RILs (1 plate for six lines, maximum=4, mean=2.0), which we consider as replicates for estimation of repeatability

(see below). In total the median number of measurements per line was 43 (range 4-84). Highly replicated data for the reference strain N2 were also included for modeling purposes (404 observations across 17 plates, spanning 9 of 47 independent thaws). Wells with no offspring were observed for 4% of N2 data (and 2.9% of all RIL data). These are likely to be due to technical artifact, such as injury or incorrect staging, and were excluded before modeling. Mapping values were the Box-Cox transformed line coefficients from a Poisson generalized linear model with fixed effects of plate row, column and edge (exterior rows and columns), and the count of offspring per worm as response variable. Three outliers with coefficients >3 standard deviations below the mean were excluded, leaving data for 227 RILs (File S4). Data come from RILs of three sub-panels (170 A6140, 45 GA50, 12 GT50), which explains 4% of trait variation (GA50 RILs have higher mean fertility than the A6140, regression coefficient = 0.43, $p = 0.01$; see [Figure S1](#)).

Adult hermaphrodite body size 412 RILs were thawed and maintained for two generations under standard conditions. On the third generation, 1000 synchronized L1 larvae were moved to NGM-lite plates (25mM NaCl) where they developed and matured for 3 days. Image data was acquired at the usual time of reproduction (as during experimental evolution) and analysed with the Multi-Worm Tracker ([Swierczek et al. 2011](#)), using a Dalsa Falcon 4M30 CCD camera and Schott backlight A08926. Tracking was performed for 25 minutes with default parameters, and particle (worm) contours extracted (on average, 300 particles obtained every 0.5s). Raw values from each plate were calculated from track segments of length 40-41s taken at 80s intervals, ultimately estimating the area of an individual as the grand mean of the per-segment estimates (accounting for temporal autocorrelation within a time-series, analysis not shown).

Assays were carried out in two lab locations over several years, while recording the relative humidity and temperature at the time of assay. Mapping values are the Box-Cox transformed line coefficients from a linear model incorporating fixed effects of year, nested within location, and humidity and temperature, nested within location. Data come from a mean of 2.1 (maximum 4) independent thaw blocks for each RIL, for 410 RILs after excluding 2 outliers >3 standard deviations below the mean, with a median of 447 measurements per RIL and block (range 109-1013; File S5). Data for the reference strain N2 were also included in the model (1664 observations from two plates). Data come from RILs of three sub-panels (165 A6140, 118 CA50, 127 GA50), which explains 17% of trait variation (GA50 RILs are much larger than the A6140, regression coefficient = 0.94, $p < 10^{-16}$; see [Figure S1](#)). This difference is not obviously associated with technical covariates, since data acquisition for A140 RILs and GA50 RILs was distributed similarly with respect to location and time.

Fertility and body size are moderately correlated ([Figure S1](#); see also [Pouillet et al. \(2016\)](#)), justifying the latter being considered a fitness-proximal trait (Spearman's $\rho = 0.354$, $p = 2.336 \times 10^{-7}$ for mapping coefficients, for 202 lines with data for both traits).

Heritability and phenotype prediction

Repeatability Repeatability was estimated from ANOVA of the line replicate means for each trait as $R = \sigma_a^2 / (\sigma_a^2 + \sigma_e^2)$, where $\sigma_a^2 = (\text{mean square among lines} - \text{mean square error})/n_0$, and n_0 is a coefficient correcting for varying number of observations (1-4 plate means) per line ([Lessells and Boag 1987](#); [Sokal and](#)

531 Rohlfs 1995). Assuming equal variance and equal proportions
532 of environmental and genetic variance among replicates, R
533 represents an upper bound on broad-sense heritability (Falconer
534 1981; Hayes and Jenkins 1997). Fertility data were square root
535 transformed to decouple the mean and variance.

536 **Assumptions** In inbred, isogenic, lines, broad-sense heritability
537 can also be estimated by linear mixed effect model from the
538 covariance between genetic and phenotypic variances. The mea-
539 surement of genetic similarity is, however, subject to a number
540 of assumptions and is (almost) always, at best, an approximation
541 (Speed and Balding 2015).

542 A first assumption is that all markers are the causal alleles
543 of phenotypic variation. It is unavoidable, however, that mark-
544 ers tag the (unknown) causal alleles to different degrees due to
545 variable linkage disequilibrium. A second, usually implicit, as-
546 sumption in calculating genetic similarity is the weight given to
547 markers as a function of allele frequency. Equal marker weights
548 have commonly been used in animal breeding research, while
549 greater weight has typically been given to rare alleles in hu-
550 man research, which has some support under scenarios of both
551 selection and neutrality (Pritchard 2002). A third assumption,
552 related to the first two, is the relationship between LD and causal
553 variation. If the relationship is positive - causal variants being
554 enriched in regions of high LD - then heritability estimated from
555 all markers will be upwardly biased, since the signal from causal
556 variation contributes disproportionately to genetic similarity
557 (Speed *et al.* 2012).

558 The use of whole genome sequencing largely addresses the
559 first assumption, given (as here) very high marker density and
560 an accurate reference genome, although in the absence of full
561 *de novo* genomes from long-read data for each individual, the
562 contribution of large scale copy-number and structural variation,
563 and new mutation, will remain obscure. To account for the sec-
564 ond and third assumptions, we used LDAK (v5.0) to explicitly
565 account for LD in the CeMEE (decay half-life = 200Kb, min-cor =
566 0.005, min-obs = 0.95) (Speed *et al.* 2012). Heritability estimates
567 were not sensitive to variation in the decay parameter over a
568 10-fold range or to the measurement unit (physical or genetic),
569 although model likelihoods were non-significantly better for
570 physical distance. Across the set of 507 RILs, 88,508 segregat-
571 ing markers were used after local LD-based pruning ($r^2 < 0.98$)
572 and, of these, 22,984 markers received non-zero weights. LD-
573 weighting can magnify the effects of genotyping errors. We
574 excluded 17,740 markers with particularly low local LD (mean
575 r^2 over a 20 marker window < 0.3 , or the ratio of mean r^2 to that
576 of the window mean < 0.3). Heritability estimates were largely
577 unchanged (within the reported intervals), as were our general
578 conclusions on variance components and model performance.

579 **Modeling** Model fit was assessed by phenotype predictions from
580 leave-one-out cross validation, calculating the genomic best lin-
581 ear unbiased prediction (GBLUP; Meuwissen *et al.* (2001); Van
582 Raden (2008); Yang *et al.* (2010)) for each RIL and returning
583 the squared correlation coefficient (r^2) between observed and
584 predicted trait values. To avoid bias associated with sample
585 size all models were unconstrained (non-error variance com-
586 ponents were allowed to vary outside 0-1 during convergence)
587 unless otherwise noted, which generally gave better fit for multi-
588 component models.

Given m SNPs, genetic similarity is calculated by first scaling
 S , the $n \times m$ matrix of mean centered genotypes, where $S_{i,j}$ is
the number of minor alleles carried by line i at marker j and

frequency f , to give X :

$$X_{i,j} = (S_{i,j} - 2f_j) \times (2f_j(1 - f_j))^{\frac{\alpha}{2}}; \quad (1)$$

The additive genomic similarity matrix (GSM) \mathbf{A} is then $\mathbf{X}\mathbf{X}^T/m$.
Here α scales the relationship between allele frequency and effect
size (Speed *et al.* 2012). $\alpha = -1$ corresponds to the assumption of
equal variance explained per marker (an inverse relationship of
effect size and allele frequency), while common alleles are given
greater weight at $\alpha > 0$. We tested $\alpha \in [-1.5, -1, -0.5, 0, 0.5, 1]$
and report results that maximized prediction accuracy. With
 Y the scaled and centered vector of n phenotype values, the
additive model fit for estimating genomic heritability h^2 is then:

$$Y = \sum^m \beta A + e,$$

with $\beta \sim \mathcal{N}(0, \sigma_g^2)$, $e \sim \mathcal{N}(0, \sigma_e^2)$

589 where β represents random SNP effects capturing genetic vari-
590 ance σ_g^2 , e is the residual error capturing environmental vari-
591 ance σ_e^2 . Given Y and \mathbf{A} , heritability can be estimated from
592 restricted/residual maximum likelihood (REML) estimates of
593 genetic and residual variance as $h^2 = \sigma_g^2 / (\sigma_g^2 + \sigma_e^2)$. Note that
594 we use the terms h^2 and genomic heritability interchangeably
595 here for convenience, although in some cases the former includes
596 non-additive covariances. We assume RILs are fully inbred, and
597 so dominance variance does not contribute to heritability.

The existence of near-discrete recombination rate domains
across chromosomes has led to characteristic biases in nu-
cleotide variation, correlated with gene density and function
(Cutter *et al.* 2009). Similarly, recent selective sweeps, coupled
with the low effective outcrossing rate in *C. elegans*, have led to a
markedly unequal distribution of variation across chromosomes
(Andersen *et al.* 2012; Rockman *et al.* 2010). This variability in
mutational effect, along with variable LD in the RILs, is not cap-
tured by aggregate genome-wide similarity with equal marker
weighting (Speed *et al.* 2012; Goddard *et al.* 2016). We therefore
first tested genetic similarity by explicitly modeling observed LD
(Speed *et al.* 2012), with markers weighted by the amount of ge-
netic variation they tag along chromosomes, and by their allele
frequency (see above). Given m weights reflecting the amount
of linked genetic variation tagged by each marker, w_1, \dots, w_m ,
the variance covariances for the basic model become:

$$\beta \sim \mathcal{N}(0, w\sigma_g^2/W)$$

where W is a normalizing constant. Second, we jointly measured
the variance explained by individual chromosomes (and by re-
combination rate domains within each chromosome), which can
further improve the precision of heritability estimation if causal
variants are not uniformly distributed by allowing variance to
vary among partitions. Third, we tested epistatic as well as addi-
tive genetic similarity with (1) the entrywise (Hadamard) prod-
uct of additive GSMs, giving the probability of allele pair sharing
(Henderson 1985; Jiang and Reif 2015), (2) higher exponents up
to fourth order interactions and (3) haplotype-based similarity
at multi-gene scale. Additional similarity components (additive
or otherwise) are added as random effects to the above model to
obtain independent estimation of variance components:

$$Y = \sum^m \beta A_1 + \dots + \beta_n A_n + e,$$

$\beta_1 \sim \mathcal{N}(w\sigma_{g1}^2 A_1 / W),$
 $\beta_n \sim \mathcal{N}(w\sigma_{gn}^2 A_n / W),$
 $e \sim \mathcal{N}(0, \sigma_e^2)$

Haplotype similarity was calculated as the proportion of identical sites among lines at 0.033 and 0.067cM scales (corresponding to means of approximately 5 and 10Kb non-overlapping block sizes, or one and two genes), using either the diallelic markers only, or all called SNPs and indels. In the latter case, variants were imputed from reconstructed haplotypes if the most likely haplotypes of flanking markers were in agreement.

GWAS

1-dimensional tests For single trait, single marker association, we fitted linear mixed models using the Python package LIMIX (<https://github.com/PMBio/limix>):

$$Y = \beta X + g + e, \text{ with } g \sim \mathcal{N}(0, \sigma_g^2 A), e \sim \mathcal{N}(0, \sigma_e^2) \quad (2)$$

where X is the matrix of fixed effects (the SNP genotype of interest) and β is the effect on phenotypic variation that is estimated. g are the random effects describing genetic covariances (as above) accounting for non-independence among tests due to an assumed polygenic contribution to phenotype, with A the $n \times n$ genetic similarity matrix from the most predictive additive fit found for each trait above, and e is the error term.

To test the mapping resolution and power of the CeMEE panel, we carried out GWAS according to the model above for simulated phenotypes. We modeled a single focal additive locus (with h^2 from 1 to 30%) and a background polygenic component of equal variance (with scenarios of 10, 100 or 1000 loci), selected at random from SNPs with MAF > 0.05, and with genetic and environmental effect sizes drawn independently from the standard normal distribution. GWAS was carried out 1000 times for each scenario, controlling for relatedness with LD-weighted additive genetic similarity ($\alpha = -0.5$). Power was estimated from a binomial generalized linear model considering all three polygenic scenarios together. Recall, the proportion of true positives passing significance, was assessed after masking a 1cM window around the focal SNP. 2-LOD drop intervals around the focal locus were calculated from similarly powered markers with \geq MAF, with p -values converted to LOD scores as $\chi^2/2 \times \log(2)/\log_{10}(2)$.

For simulated traits all 507 lines and 262,218 markers (MAF > 0.05) were used for GWAS. For body size GWAS 410 lines and 254,174 markers were used, and 227 lines and 254,240 markers were used for fertility. Significance thresholds were established by permutation, with phenotypes generated by permuting phenotype residuals, given the estimated relatedness among lines (A), using the R package mvnpermute (Abney 2015). Significance level α is the corresponding percentile of the minimum p -values from 1000 permutations.

Given the correlation between traits (see above), we also tested a model for each trait on phenotype residuals after linear regression on the other, and a multi-trait model fitting effects common or specific to a trait. No markers passed significance in any case (analysis not shown).

2-dimensional tests We tested for additive-by-additive epistasis on the assumption of complete homozygosity. We first reduced the search space by local LD pruning ($r^2 < 0.5$), requiring MAF > 0.05, the presence of all four two-locus homozygote classes at a frequency of ≥ 3 , with ≤ 5 missing or ambiguous imputed genotypes (which were excluded from analysis). This gave a total of 19,913,422 tests for fertility (both inter- and intrachromosomal) and 28,138,090 for size, across 9,628 and 10,329 markers respectively. We tested for main and interaction additive effects

for all marker pairs by ANOVA, taking as summary statistics the F -statistic for genotype interaction (2D tests), and also the sum of interaction scores for each marker (2D sum tests) above each of three thresholds ($F > 0, 8, 16$, the latter corresponding roughly to the most significant single marker associations seen for both traits). All statistics were calculated separately for inter- and intrachromosomal tests. 2D sum tests are testing for excess weak to moderate interactions due to polygenic epistasis.

For computational tractability, tests were run in parallel on two chromosomes at a time. Null permutation thresholds were generated by shuffling phenotypes (using mvnpermute as above to ensure exchangeability in the presence of polygenicity or structure). 2D test thresholds were calculated for each chromosome separately from at least 2000 permutations each and differed little across chromosomes ($\alpha = 10\%$, $2.86 - 1.16 \times 10^{-7}$ for fertility, $1.86 \times 10^{-7} - 7.2 \times 10^{-8}$ for size). Inter- and intrachromosomal thresholds were calculated separately, but the reported interactions do not change if we pool both classes (or all chromosomes). 2D sum test thresholds were calculated separately for each chromosome pair and class (inter- and intrachromosomal).

We initially ignored relatedness for 2D testing, then fit linear mixed effect models as above with genetic covariance A for candidate interactions (R package hglm; Shen *et al.* (2014)). For size, the two candidate interactions all decreased slightly in significance (to a maximum p -value of 7.8×10^{-7}), while significance increased for all four fertility interactions. The amount of phenotypic variance explained by candidates for each trait was estimated by ANOVA, jointly fitting all main and two-locus interactions.

Data Availability

Sequence data are available from NCBI SRA under accession XXXXX. All data and methods scripts are archived in Dryad.org doi: XXX. RILs are available from the authors.

Results and Discussion

CeMEE differentiation from natural populations

The CeMEE panel of recombinant inbred lines draws variation from sixteen founders, and shuffles the diversity they contain through more than 150 generations at moderate population sizes and predominant outcrossing. The wild founders used to create the panel together carry approximately 25% of single nucleotide variants known to segregate in the global *C. elegans* population (CeNDR; *Caenorhabditis elegans* Natural Diversity Resource; Cook *et al.* (2017)). They vary, however, in distance to the N2 reference strain, with the Hawaiian CB4856 and German MY16 isolates together contributing over half of all markers, while the Californian CB4507 is closely related to N2 (Figure S3). Comparison of pairwise genetic distances in the CeMEE and 152 sequenced wild isolates (including a small number of more recently isolated, highly divergent lines) illustrates the extent of novelty generated by the multiparental cross (Figure 2). The CeMEE RILs occupy a substantial sub-space of the CeNDR genotypic diversity (Figure 2A), without the extensive haplotype sharing among wild-isolates and with the creation of many new multi-genic haplotypes (Figure 2B).

CeMEE differentiation from parental founders

Since *C. elegans* natural isolates suffer from outbreeding depression (?Gimond *et al.* 2013), the mixing phase is expected to generate high variance in fitness which, channeled through

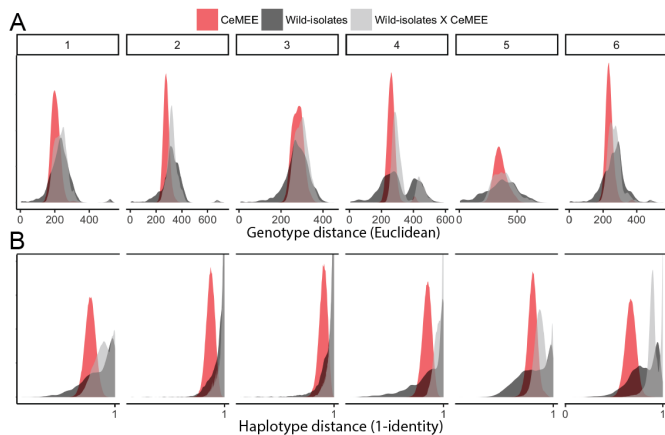


Figure 2 Similarity among CeMEE RILs and 152 sequenced wild-isolates (*Caenorhabditis elegans* Natural Diversity Resource) at 256,535 shared diallelic sites. The distribution of pairwise genotype (A) and haplotype (B) distances, within and between CeMEE RILs and CeNDR wild-isolates, by chromosome. Haplotype distances are 1-% identity at 0.1cM scale. Note that chromosomes 2-4 all show a marked excess in haplotype dissimilarity between CeMEE RILs and CeNDR wild-isolates, and the density is truncated by a factor of four for visibility.

746 of alleles more generally. These effects are expected to depend
747 on reproductive mode and selection (Charlesworth and Wright
748 2001; Morran *et al.* 2009; Chelo and Teotónio 2013; Chelo *et al.*
749 2014; Kamran-Disfani and Agrawal 2014) and will be addressed
in future work.

711 bottlenecks during serial intercrossing and population expansion,
712 gives ample opportunity for loss of diversity through drift
713 and selection. Fixation of N2 alleles at one X chromosome locus,
714 spanning the known major effect behavioral locus *npr-1* (de Bono
715 and Bargmann 1998; Gloria-Soria and Azevedo 2008; McGrath
716 *et al.* 2009; Reddy *et al.* 2009; Andersen *et al.* 2014; Bendesky *et al.*
717 2011), during establishment of the A140 population has been
718 documented with a coarse marker set (Teotónio *et al.* 2012). More
719 broadly, the outbred A140 population showed non-negligible
720 departure from the founders, with 32,244 alleles lost (unseen in
721 both the A140 and RILs, 26,593 of these being founder single-
722 tons; Figure 3). Subsequent change during the inbreeding (and
723 further adaptation) stages to generate RILs was more restricted,
724 with an additional 3,171 alleles lost (2,542 of these at <10% fre-
725 quency in both founders and the A140). Importantly, however,
726 the physical distribution of allelic loss is relatively restricted:
727 at least one marker is segregating in the CeMEE RILs at >5%
728 minor allele frequency within 95.5% of 20Kb segments across
729 the genome (97.2% of autosomal segments; for reference, protein
730 coding genes are spaced just under 5Kb apart on average in the
731 100Mb *C. elegans* N2 genome).

732 Analysis of differentiation across variant functional classes
733 showed large departures in frequency for coding variation
734 (synonymous and non-synonymous) and the smallest for intron-
735 ic variation (Figure 3D). Putative regulatory variation was
736 most variable across experimental phases, being the most dynam-
737 ic class during the funnel intercross and initial adaptation
738 (founders to A140) but below the mean value for generations
739 between the A140 and RILs. This pattern was observed across
740 all of the sub-panels that make up the CeMEE (not shown), not-
741 ably the A140 RILs which differ from the outbred A140 by only
742 inbreeding, suggesting differential dominance of coding and
743 regulatory variation (Wray 2007; Gruber *et al.* 2012). Without
744 sequence data for the outbred CA50, GA50, GM50 or GT50 popu-
745 lations, we cannot assess the impact of inbreeding on the fixation

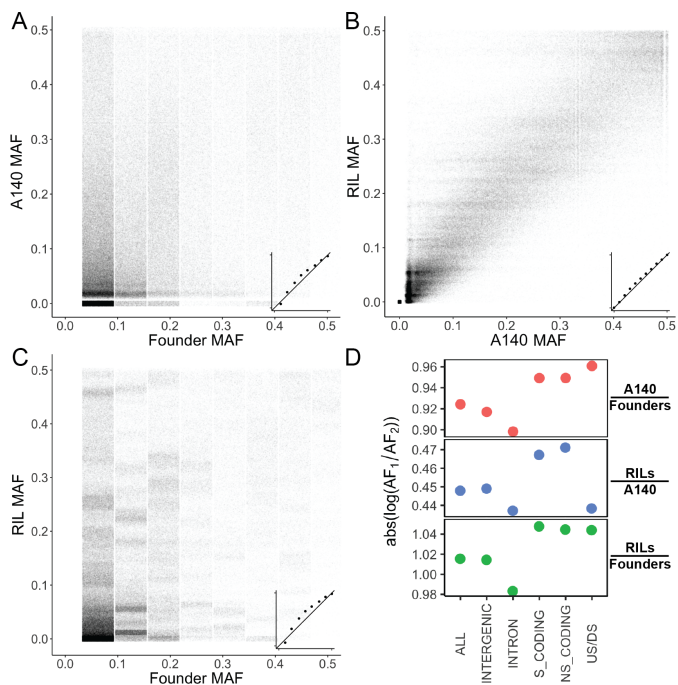


Figure 3 Minor allele frequency between founders and the outbred A140 population (A), A140 and RILs (inbreeding only for the A140 RILs, further adaptation then inbreeding for G50 RILs; B), and founders against all RILs (C). Insets show frequency quantiles. D. Change in allele frequency (absolute log ratios) for the same contrasts by functional class: intronic, synonymous and non-synonymous, putative regulatory variation (US/DS; ≤ 200 bp from an annotated transcript or N2 pseudogene), or intergenic (none of the above). Points are mean values (diameter exceeds the standard errors).

750 Local linkage disequilibrium, while non-uniform among chromo-
751 somes, decays relatively rapidly on average, approaching
752 background levels by 0.5cM (F_2 map scale) on average (Fig-
753 ure 4 and Figure S2). Disequilibrium between pairs of loci on
754 different chromosomes is, as expected, very weak (0.99, 0.95
755 quantiles = 0.538, 0.051 within chromosomes versus 0.037, 0.022
756 across chromosomes), with the prominent exception of a single
757 pair of loci on chromosomes II and III ($r^2 > 0.5$ between
758 II:2,284,322; tagging an intact MARINER5 transposon (WBTrans-
759 poson00000128) that harbors an expressed miRNA in the N2
760 reference, and III:1,354,894-1,425,217; a broad region of mostly
761 unannotated genes, against maximum interchromosomal values
762 for all other pairs $r^2 \leq 0.27$). Alleles in repulsion phase are rare
763 across these regions ($p < 10^{-70}$, Fisher Exact Test), absent in the
764 founders, and present in only 1 of 124 wild isolates surveyed
765 with unambiguous variant calls in these regions (*Caenorhabditis*
766 *elegans* Natural Diversity Resource). This suggests the presence
767 of at least one two-locus incompatibility exposed by inbreeding
768 or, perhaps more likely given the uncertainties of reference-
769 based genotyping, a transposon-mediated II-III transposition
770 polymorphism among founders. Three founders contribute the

772 chromosome II non-reference haplotype, but extremely poor
773 read mapping in this region for these and other isolates, consis-
774 tent with high local divergence as well as potential structural
775 variation, means our short read data are not informative in res-
776 solving these alternatives.

777 To better quantify the extent of subtle interchromosomal
778 structure in the CeMEE we compared the observed correlations
779 among chromosomes to values from permutations, shuffling
780 lines within sub-panels, among chromosomes (Figure 4). The
781 observed mean value for the genome, while extremely low, is
782 highly significant ($p < 2 \times 10^{-4}$ from 5000 permutations), indi-
783 cating the presence of extensive weak interactions. Further
784 permutations dropping single or pairs of chromosomes showed
785 that interactions between autosomes and the X chromosome
786 contribute disproportionately.

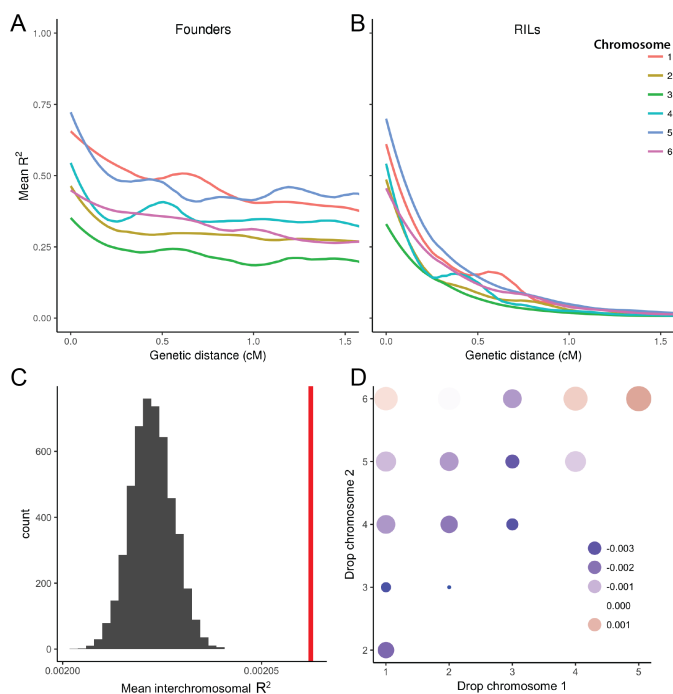


Figure 4 Linkage disequilibrium in founders (A) and all CeMEE RILs (B; F_2 genetic map distance, LOESS fit to mean r^2). C. Interchromosomal structure is weak but significant. Observed mean r^2 across all chromosomes (red vertical bar) plotted against the null distribution from permutations randomizing lines across chromosomes (within sub-panels to exclude effects of population structure). D. Permutations dropping pairs of chromosomes implicate X-autosome interactions. Point size and color is scaled by enrichment over the null distribution (95% percentile), relative to the genome-wide mean value.

787 Founder haplotype blocks and genetic map expansion

788 The CeMEE panel is highly recombined and any simple, large-
789 effect incompatibilities between founders are likely to have been
790 purged. For example, a haplotype containing *peel-1* and *zeel-1*, a
791 known incompatibility locus that segregates among the founders
792 on the left arm of chromosome I (Seidel *et al.* 2008, 2011), is fixed
793 in the RILs (Figure 5a). Cases such as this are best appreciated
794 when the mosaic of founder haplotypes across the genome is
795 inferred.

796 For each CeMEE RIL, founder haplotypes across the genome
797 were reconstructed with the multiparent HMM framework RAB-
798 BIT (Zheng *et al.* 2015), assigning 96.9% of markers to a single
799 founder haplotype at posterior probability > 0.2 ($84.2\% > 0.5$;
800 median value across lines). Haplotype sharing in the 16 founders
801 means that unambiguous assignment to a single founder is not
802 always possible). For illustration purposes, a summary of re-
803 constructed haplotypes for the A140 RILs on chromosomes I,
804 IV and X are shown in Figure 5, at both physical and genetic
805 scales to make the differences between these units plain. The
806 observed recombination landscapes generally recapitulate those
807 inferred from the N2/CB4856 cross (Rockman and Kruglyak
808 2009; Kaur and Rockman 2014; Bernstein and Rockman 2016),
809 with recombination rate high in chromosome arms and low in
810 centers. With the additional map expansion gained here (see
811 below), we note that suppression of recombination is clearly
812 strong, but not complete, within subtelomeric regions (see, for
813 example, the exceptionally large right tip of chromosome X,
814 spanning almost 2Mb, in Figure 5c).

815 Founder haplotype diversity among all CeMEE RILs remains
816 high: the median number of founder haplotypes across recon-
817 structed intervals is 12 (posterior probability > 0.5 , haplotypes
818 observed in > 1 RIL). Contributions clearly vary from equality,
819 with lines most divergent from the reference (CB4856 and
820 MY16) overrepresented and lines more similar to the reference
821 underrepresented (with the exception of the large region of chro-
822 some X, spanning *npr-1*, which is largely fixed for N2/CB4507
823 alleles (Figure 5c). To establish if these biases are merely techni-
824 cal, and establish expectations for reconstruction resolution in
825 the presence of haplotype redundancy, we simulated genomes of
826 varying pedigree length (up to 150 generations). As expected,
827 reconstruction was hampered by increasing recombination, and by
828 ambiguity between similar founders (Figure S3). Bias toward di-
829 vergent haplotypes was not observed in the reconstruction simu-
830 lations, however, suggesting the overrepresentation of CB4856
831 and MY16 may be due to selection, notably for long haplotypes
832 across the central domain of chromosome IV (Figure 5b). Re-
833 construction completeness for the A140 RILs is generally in line
834 with expectations for a pedigree of 150 generations. Clear excep-
835 tions are chromosome IV, where we recover more than expected
836 under random sampling, and chromosome V, where we recover
837 less. Haplotype lengths from simulated reconstructions showed
838 we progressively underestimate recombination breakpoints due
839 to imperfect resolution of small haplotypes (Figure S3).

840 The relationship between known generation and estimated
841 realized map expansion from reconstruction simulations allows
842 prediction of the number of effective generations of outcrossing
843 within the CeMEE panel. Across the five sub-panels, mean
844 autosomal generation ranges from 227 (GM monoecious RILs)
845 to 284 (CA androdioecious lines), with a weighted average of
846 260 for the CeMEE as a whole (Figure S4). Estimated genetic
847 map expansion is variable across chromosomes: IV appears to
848 be exceptionally recombinant in all sub-panels with expansion
849 more than twice that of chromosomes I-III, due largely to a high
850 frequency, highly structured haplotype on the far right arm and
851 tip (Figure 5b). This region spans one of the two large *C. el-*
852 *egans* piRNA clusters (Ruby *et al.* 2006), which encodes more
853 than 15,000 piRNA transcripts, interspersed with active trans-
854 posons and protein coding genes. Several trivial explanations
855 for the unusual apparent expansion, such as elevated genotyp-
856 ing error rate or founder haplotype ambiguity, or distortions
857 in the N2/CB4856 genetic map use to condition reconstruction

probabilities, are not supported (data not shown), although the extent of large-scale structural variation among founders in this region (with the exception of CB4856, which does not show unusual levels of SNP or copy number variation) is unknown. Setting aside potential technical artifacts, the locus may represent a hitherto undetected recombination hotspot (whether through attraction, or suppression of observed recombination elsewhere on the chromosome), a site of rampant gene conversion, or the focus of early and sustained selection during the initial intercross phase (potentially epistatic in nature, see [Neher and Shraiman \(2009\)](#)). Earlier work proposed that evolution of this region may have involved a recombination rate modifier (through gene conversion) during the first 140 generations of experimental evolution in order to explain the observed excess haplotype diversity (see discussion and Figures S4 and S5 of [Chelo and Teotónio \(2013\)](#)). In contrast, chromosome V, which has been the focus of a recent large-scale selective sweep ([Andersen et al. 2012](#)), shows more variable expansion across sub-panels suggestive of ongoing selection ([Figure S4](#)).

Population stratification

We examined additional genetic structure in the CeMEE RIL panel stemming from the inclusion of distinct sub-panels of RILs that vary in experimental evolution histories. In the context of QTL mapping, this genetic structure represents nuisance variation that can bias estimates of heritability if unknown factors covary with the trait of interest, structure that is causally associated with a trait, or non-causal structure due solely to population stratification.

To gauge the extent of population stratification we compared the results of supervised and unsupervised discriminant analysis of principal components (DAPC; [Jombart \(2008\)](#)), which partitions within and between group variation, using either known or inferred populations, based on linear combinations of principal components. By selection of discriminant functions that best predict known CeMEE sub-panel membership, it is clear that the varied evolutionary history has, unsurprisingly, generated significant genetic structure. The number of principal components selected by cross-validation that best predicts population membership is 40, which together explain 25% of the variance (though only a fraction of these components are significantly associated, considered singly or in pairs, see [3](#)). Unsupervised DAPC, which infers groups based on variance minimization and model penalization criteria (k -means clustering, BIC), selected 5-8 clusters which best explain the data (Δ BIC < 1 over this range). These corresponded significantly with sub-panel identity (e.g., $p = 0.036$ at $k=5$, permutation test), although the rate of successful assignment was low (36% at $k=5$). This suggests that genetic structure within, as well as between sub-panels, is significant.

Heritability and predictability of fitness-proximal traits

We measured two traits that are important components of fitness – the fertility and size of young adult hermaphrodites – and thus represent challenging case studies for mapping of complex traits in the panel ([Pouillet et al. 2016](#)). The traits are correlated ([Figure S1](#)), and vary extensively in the CeMEE RILs: hermaphrodite fertility varies more than five-fold, size varies more than three-fold ([Figure 7](#)).

Under the uncommonly met assumptions of complete tagging of causal variation and uniform linkage, narrow sense heritability (h^2) can be estimated from phenotypic and additive genetic covariances ([Henderson 1975](#); [Robinson 1991](#); [Yang et al.](#)

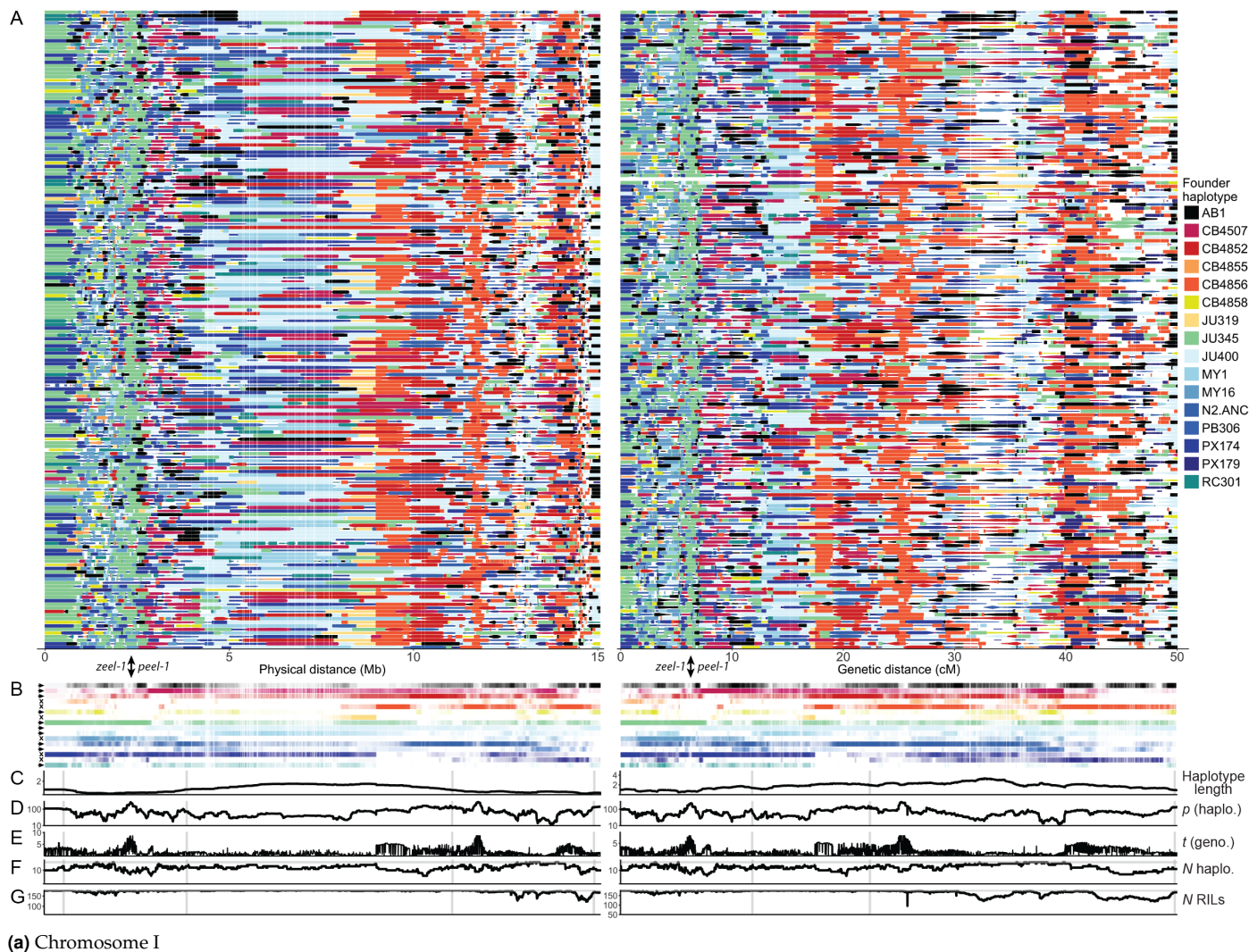
[2010](#); [Speed et al. 2012](#); [de los Campos et al. 2015](#)). Estimates, assuming appreciable heritability, are influenced by the extent to which markers reflect the genetic architecture of the trait in the population under study, and the method by which similarity is defined from them (reviewed in [Speed and Balding \(2015\)](#), and see [Materials and Methods](#)). Different covariance metrics can therefore provide useful information on the genetic basis of complex traits, such as partitioning chromosomal contributions, the frequency distribution of causal variants, and the proportion of epistatic variance, without the statistical limitations (and precision) of GWAS that attempt to explain phenotypic variance as the sum of individually significant additive marker effects. As emphasized by [Speed and Balding](#), genomic heritability estimation is best viewed as a model-fitting exercise, the problem being to find the most appropriate measure of genetic similarity for the trait, population and genetic data in question, and the answer being the most likely estimate of the contribution of genetic variance to trait variance given the data.

Repeatability, genomic heritability and prediction While RIL repeatability (an upper bound on broad sense heritability, H^2 , under certain assumptions ([Dohm 2002](#))) for both traits was relatively high – 0.76 for fertility and 0.80 for size – genomic heritability estimates for trait coefficients with a simple additive genetic similarity matrix based on the probability of allele sharing at all markers, equally weighted, were not significantly different to 0 (likelihood ratio test; not shown). This suggested that genome-wide genotypic similarity is poorly correlated with causal variation for these traits, potentially due to variable LD or epistatic cancellation. We thus examined alternative measures of genetic similarity to address the apparent lack of additive genomic heritability, comparing model predictive power (r^2) by leave-one-out cross-validation (see [Materials and Methods](#)).

Heritability estimates and prediction accuracy are summarized in [Table 1](#), comparing the simplest models – additive (A) only, or additive + additive-by-additive (A^2) genetic covariance at the genome level – and the most predictive models for each trait. Given relatively high variance in relatedness, we are powered to detect large differences in additive heritabilities despite modest sample sizes for analysis of this kind, although the differences between individual models are generally minor. For fertility, with just 227 lines we have 50% power to reject $h^2 = 0$ if $h^2 = 0.38$, and >95% power at our estimate of H^2 (at a significance level of 0.05), while for size, the corresponding values are 50% power at $h^2 = 0.35$ and >99% power at repeatability (based on the best performing measure of additive similarity for each trait; [Visscher et al. \(2014\)](#)). Given the multiplicative scaling of epistatic similarity, low power is unavoidable.

While phenotype prediction accuracy is generally poor, some broad trends are apparent in the ranking. Additive heritability based on LD-weighted markers was relatively high for size (0.58), though less so for fertility (0.24). In neither case was additive similarity alone the best predictor of phenotype, however. Nine of the top 10 models for fertility all incorporated epistasis in some form, with the best of these giving 57% improvement over the best additive model. For size, the advantage was less clear: three of the top four models included epistasis, though the performance differential between the best epistatic and additive models was only 3%.

Notably, partitioning of the genome based on recombination rate domains performed well for both traits, and was the preferred model for fertility. In general, model type was more influential on prediction than allele frequency scaling (α), how-



(a) Chromosome I

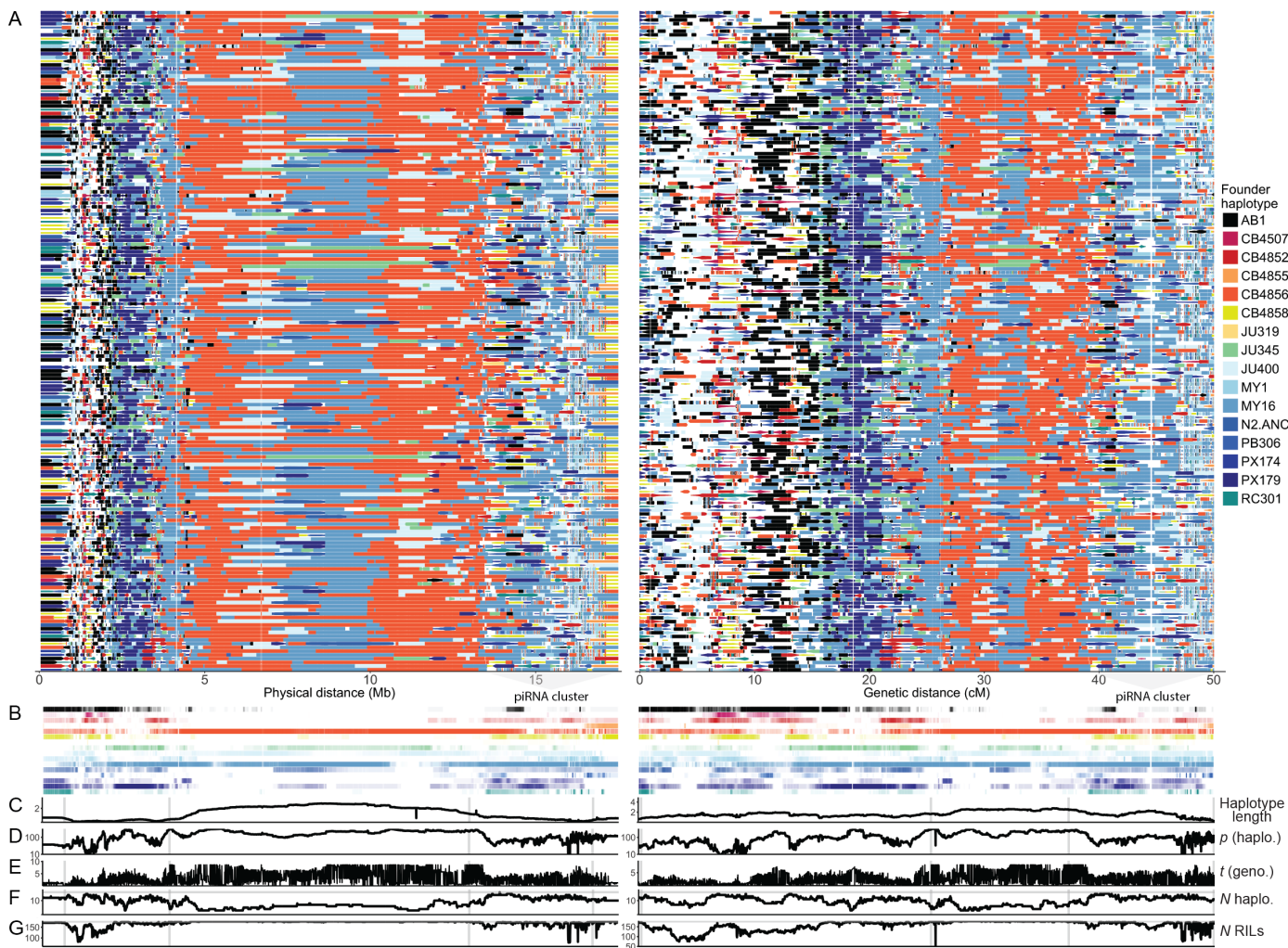
Figure 5 A140 RIL founder haplotype reconstruction and structure for chromosomes I, IV and X. **A.** Founder haplotypes reconstructed for the A140 RILs shown in physical and genetic distances. Each plotted point is a marker, with its size scaled by posterior probability (minimum 0.2). Founder contributions are summarized below in **B.** Loci discussed in the text are indicated: the *zeel-1/peel-1* incompatibility on the left arm of chromosome I (haplotype compatibility group, either experimentally tested in [Seidel et al. \(2008\)](#) or determined here from genotype data, is indicated below as an arrowhead for Bristol (N2) or an x for Hawaii (CB4856); extreme haplotype differentiation within a piRNA cluster on the right arm and tip of chromosome IV; and the fixation of N2/CB4507 haplotypes over a large region of the X chromosome left arm spanning *npr-1*, which has known pleiotropic effects on behavior and laboratory adaptation ([de Bono and Bargmann 1998](#); [Gloria-Soria and Azevedo 2008](#); [McGrath et al. 2009](#); [Andersen et al. 2014](#)). **C-G** show summary statistics evaluated at 5Kb or 0.01cM resolution, with vertical scales for each metric fixed across chromosomes, and the positions of recombination rate boundaries inferred for the N2×CB4856 RIALs ([Rockman and Kruglyak 2009](#)) indicated with shaded bars. **C.** Haplotype length; mean length extending from the focal position. **D.** p (haplo.); test of reconstructed founder haplotype proportions, relative to expectation based on reconstruction frequency from G_{150} simulations ($-\log_{10}(p)$ from a χ^2 goodness-of-fit test). **E.** t (geno.); change in allele frequency from the founders (absolute value of Welch's t statistic for founder vs. RIL genotype counts). **F.** N haplo.; the number of unique founder haplotypes detected at each position, with the maximum value of 16 indicated. **G.** N RILs; the number of RIL haplotypes reconstructed at each interval (> 0.2 posterior probability), with the maximum value of 178 indicated.

980 ever within models, negative values of α (rarer alleles having
981 larger effects) were generally preferred for size, and positive for
982 fertility, suggesting the frequency spectrum of causal variants
983 for the two traits varies in the RILs.

984 **Effects of population stratification on heritability estimation**
985 Given the stratified nature of the CeMEE panel, we tested for ef-
986 fects on heritability estimation in three ways. First, we estimated

987 heritability for individual sub-panels (best additive models only).
988 Although highly uncertain given the very small sample sizes,
989 estimates were positive for two of the three sub-panels for adult
990 body size and for both of two sub-panels tested ($n > 50$) for
991 fertility, spanning the reported values for all lines.

992 Second, we estimated within sub-panel heritability by fitting
993 within population means as covariates (best **A** and **A+A²** mod-



(b) Chromosome IV

994 els). For adult body size, where GA RILs are significantly larger
 995 than other panels, this reduced estimated heritability to 0.15 (A)
 996 and 0.38 ($A+A^2$, with $A^2=0.30$). Fertility, for which trait values
 997 vary only weakly with sub-panel, was largely unchanged at 0.45
 998 (A) and (the unreasonably high, and uncertain) estimate of 1.44
 999 (SD 0.75) for $A+A^2$, with a dominant contribution from epistasis.

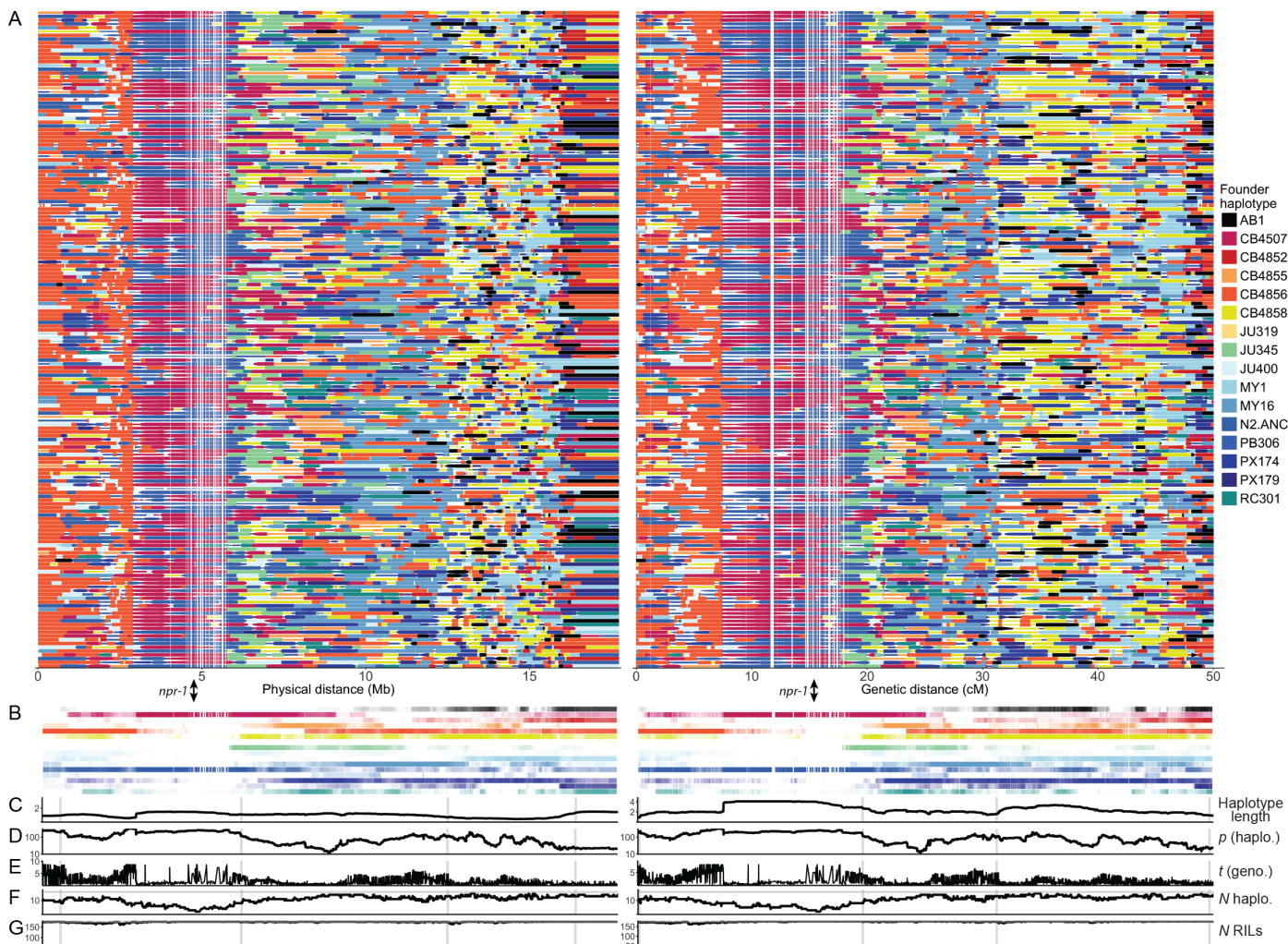
1000 Third, we applied the method of Yang *et al.* (2011), developed
 1001 for unrelated human populations, which compares the sum
 1002 of heritabilities estimated for single chromosomes to that of a
 1003 model fitting all chromosomes jointly. In the former case, genetic
 1004 correlations across chromosomes due to population structure
 1005 will result in $\sum h^2_{C(single)} > h^2_C$, since the genotype of one chro-
 1006 some will be predictive of that of others, while fitting all
 1007 chromosomes jointly gives independent conditional estimates.
 1008 The reasonable underlying assumptions are that structure is
 1009 more significant between than within populations, and is not
 1010 causally associated with phenotypic variance, although the latter
 1011 might not hold for fitness-proximal traits. Comparing the sum
 1012 of heritability estimates from samples of half the chromosomes
 1013 ($\sum h^2_{/2}$) to that from all chromosomes (additive similarity only),
 1014 results suggested stratification may contribute significantly to
 1015 our estimates for size, with mean $\sum h^2_{/2}=0.72$ (contributing 20%
 1016 of the total given $h^2=0.60$ for a joint chromosome model), but not
 1017 for fertility (mean $\sum h^2_{/2} < h^2$). Fitting up to 80 principal compo-

1018 nents as covariates for size failed to bring this ratio to equality,
 1019 but progressively eroded the heritability estimate (minimum
 1020 10% inflation for 80 PCs, $h^2=0.30$), while fitting three DAPCs
 1021 (based on the top 40 PCs) fully accounted for the difference
 1022 (mean $\sum h^2_{/2} = h^2 = 0.39$). Notably, performing the same analy-
 1023 sis within sub-panels, however, gave a similar level of ‘inflation’
 1024 for size within the largest group of RILs (28%), suggesting that
 1025 structure not associated with sub-panel is also influential.

1026 The above analyses lead us to conclude that results presented
 1027 in Table 1 for fertility are robust, while those for adult size are
 1028 somewhat less so. The extent of inflation, however, is unlikely
 1029 to be as severe as indicated by disjoint genome partitioning, and
 1030 no covariates were fit for subsequent analyses.

1031 GWAS

1032 **QTL mapping power and precision** We first explored the char-
 1033 acteristics of the CeMEE panel relevant to mapping quantitative
 1034 traits. We carried out association tests by linear mixed effects
 1035 model on simulated phenotypes, varying the effect size of causal
 1036 variation and the degree of polygenicity (see [Materials and Meth-](#)
 1037 [ods](#)). The panel reaches 50% power for an allele explaining 0.047
 1038 of the phenotypic variance (permutation 5% significance thresh-
 1039 old of $p < 1.62 \times 10^{-6}$), with recall (% true positives) greater than
 1040 50%, (Figure 6). When detected, the median QTL support inter-



(c) Chromosome X

1041 val (a drop in LOD of 2) spans < 10Kb for variants explaining
 1042 >2.5% of trait variance. Given an average gene size of approxi-
 1043 mately 5Kb in *C. elegans* N2, including intergenic sequence, the
 1044 CeMEE reaches sub-genic resolution for alleles of moderate ef-
 1045 fect (>10%), yielding high mapping precision (Figure 6). We note
 1046 that our simulations are unbiased with respect to chromosomal
 1047 location, while causal variation for many traits may be enriched
 1048 on the highly recombinant arms, so these estimates are likely to
 1049 be conservative.

1050 **1D mapping of fertility and size** We carried out single marker
 1051 genome-wide association tests by linear mixed effects model,
 1052 controlling for genome-wide relatedness using the most predic-
 1053 tive LD-weighted additive genetic similarity matrix for each
 1054 trait (see above). Based on permutation thresholds, no single
 1055 marker reached significance in either case ($\alpha = 0.1$ thresholds
 1056 = 4.38×10^{-6} and 5.57×10^{-7} for size and fertility, with mini-
 1057 mum observed p -values of 2.8×10^{-5} and 7.23×10^{-5} respec-
 1058 tively; Figure 7). For size, p -values were moderately inflated
 1059 at the high end, with a number of regions approaching signifi-
 1060 cance, but were strongly deflated for fertility, consistent with
 1061 model misspecification. Results were largely independent of
 1062 the method used to define similarity or, for fertility, whether
 1063 correction for relatedness was applied at all (Figure S5). LD
 1064 score regression, a related approach that explicitly assumes an

1065 infinitesimal architecture (Bulik-Sullivan *et al.* 2015), gave fur-
 1066 ther support for extensive polygenicity with effects distributed
 1067 across the genome (again, mostly clearly for fertility; Figure S6).
 1068 Given significant heritabilities for both traits, and the results
 1069 of GWAS simulations, the absence of individually significant
 1070 associations suggests architectures comprising many variants
 1071 with additive effects explaining <5% of the phenotypic variance.

1072 **2D mapping of additive-by-additive interactions** Given sugges-
 1073 tive evidence for epistasis from variance decomposition and a
 1074 lack of individually significant additive effects by 1D mapping,
 1075 we sought to identify interactions by explicitly testing pairs of
 1076 markers. As summary statistics we retained the ANOVA inter-
 1077 action F statistic, as well as the sum of values for each marker
 1078 across all tests for a chromosome pair (thresholded at $F > 0, 8$ and
 1079 16, the latter corresponding approximately to the most signifi-
 1080 cant 1D associations seen). At a significance level of $\alpha = 0.1$ we de-
 1081 tect four interactions (between seven loci) for fertility and two for
 1082 size, with modest marginal additive effects (Figure 8; best single-
 1083 locus statistics per pair ranging $p = 9.1 \times 10^{-3} - 9.9 \times 10^{-5}$ for
 1084 fertility and $p = 1.1 \times 10^{-3} - 9.9 \times 10^{-6}$ for size). The variance
 1085 explained by each pair, considered individually, is high: 12-15%
 1086 for fertility and 7-8% for size, and a joint linear model explains
 1087 32% and 15% of the phenotypic variances.

1088 By summing interaction scores in 1-dimensional space to test

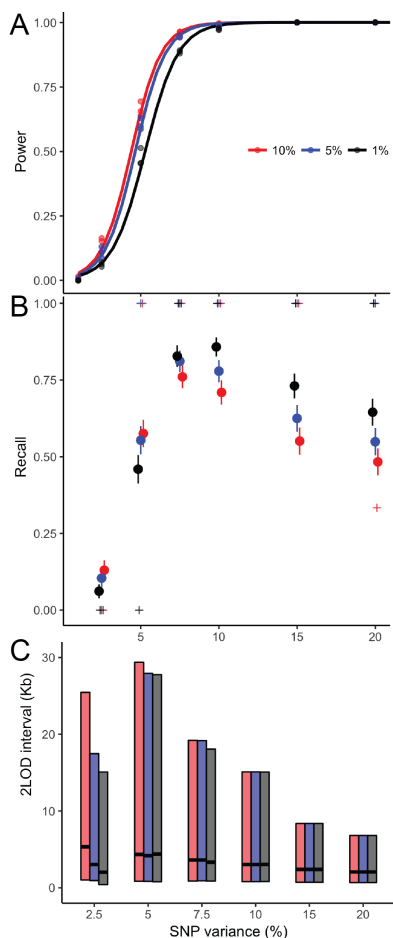


Figure 6 Additive QTL mapping simulations. Detection power (A), recall (B) and resolution (C; 2-LOD drop interval size for detected QTL) from single QTL simulations for the full mapping panel of 507 lines, as a function of detection threshold (significance at 0.01, 0.05 and 0.1) and phenotypic variance explained by the simulated QTL. Total heritability of simulated phenotypes is twice that of the focal QTL, with the polygenic contribution spread over 10, 100 or 1000 background markers (plotted in A, combined in B and C). In B, points are mean \pm standard error. Recall declines with SNP variance at high levels as chance associations reach significance, although the median value (+ symbols) is 1.0 at 5% significance for variants that explain $\geq 7.5\%$ of trait variance.

Table 1 Genomic heritability estimates

Trait	GSM	α	r^2	\hat{h}^2 (SD)	LR
Size	A	-0.5	0.073	A 0.58 (0.14)	10.8
	A+A²	-0.5	0.093	A 0.57 (0.15)	10.9
	A²			A² 0.21 (0.51)	
Fertility	A	1	0.012	A 0.24 (0.24)	0.01
	A+A ²	1	0.029	A 0.36 (0.21)	2.67
	(A+A²)_{rec}	1	0.064	A_{arm} 0.44 (0.18)	6.98
			A_{cen.} 0.02 (0.07)		

Results are shown for additive (A) and additive-by-additive (A²) genetic similarity matrices (GSM), and for the most predictive model tested (if neither of the above), shown in bold. α is the scaling parameter from (Speed *et al.* 2012), which determines the effect size expectation for markers as a function of allele frequency, where 0 is unweighted and smaller values assign greater weight to rare alleles. Unconstrained REML estimates and standard deviations are shown for components that were >0 at convergence. LR is improvement over the null model (likelihood ratio). A+A²_{rec} is additive and additive-by-additive similarity at the level of recombination rate domains (tips, arms and central domains).

1089 for polygenic epistasis, we detect 10 unique markers with ex-
 1090 cess interchromosomal interactions for 3 chromosome pairs for
 1091 fertility ($\alpha=0.1$, across all three minimum F threshold classes),
 1092 and one for size (at $F>0$; Figure 8). Only one of these sites also
 1093 reaches significance in single pair tests: position 1,914,315 on
 1094 chromosome IV, which is involved in individually significant
 1095 interactions of opposite effect with chromosome II and III for
 1096 fertility, and, remarkably, has at least one interaction of weak
 1097 to moderate effect ($10^{-5} < p < 10^{-4}$) with all other chromo-
 1098 somes. A flanking marker in modest linkage disequilibrium
 1099 (IV:1,894,021, $r^2 = 0.31$) also shows a significant excess of in-
 1100 teraction scores with chromosome III that do not appear to be
 1101 driven solely by LD: 6/12 interactions ($F > 16$ for IV:1,894,021)
 1102 are shared with IV:1,914,315, and among all 26 interactions in-
 1103 volving these two sites ($F > 16$ for either), interactions statistics
 1104 are uncorrelated ($r = -0.15, p = 0.49$). Nevertheless, experi-
 1105 ment will be required to test these loci independently.

1106 IV:1,914,315 is found within an intron of *egl-18* (encoding a
 1107 GATA transcription factor), while IV:1,894,021 falls within the
 1108 large intergenic region between *egl-18* and *egl-4* (encoding a
 1109 cyclic-GMP-dependent protein kinase thought to act in the TGF-
 1110 beta pathway), both of which vary in coding and UTR sequence
 1111 among founders, and have numerous known phenotypes from
 1112 classical induced mutations and RNAi spanning the gamut of
 1113 behavior, development and reproduction. Their eponymous phe-
 1114 notype, egg-laying abnormal (Egl), is retention of oocytes and
 1115 embryos, a phenotype selected during experimental evolution
 1116 in which embryos were extracted each generation by bleaching
 1117 (Pouillet *et al.* 2016).

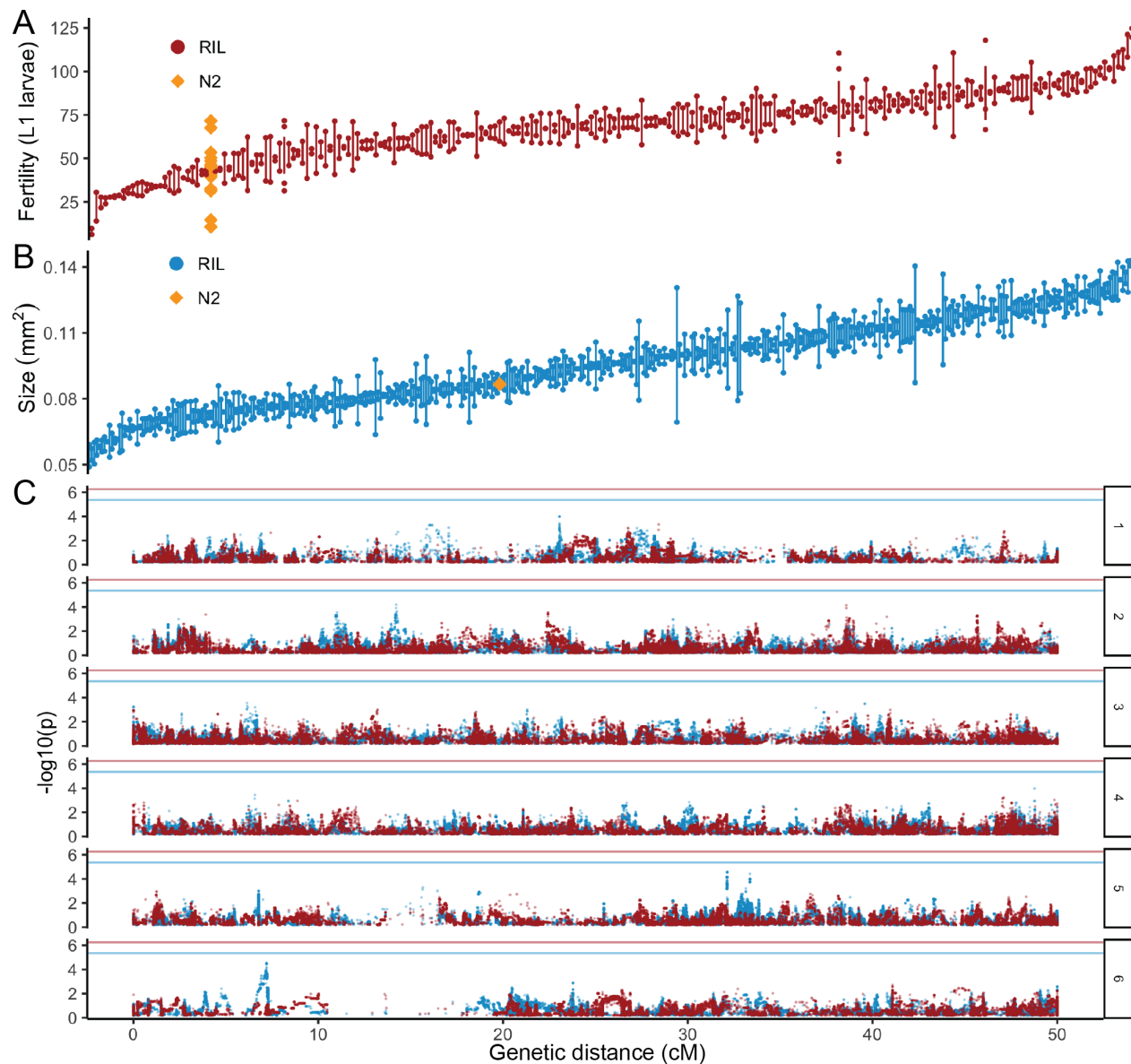


Figure 7 1D GWAS. **A-B.** Trait value distributions across RILs (replicate means; bars show data range or the standard error for samples with >2 replicates) and **(C)** single-SNP association results for fertility and adult body size (colors as above). Values for the reference N2 strain are shown for comparison. Note that values are raw replicate means on the original scale, and so include all sources of technical variation (unlike model coefficients used for mapping).

CONCLUSIONS

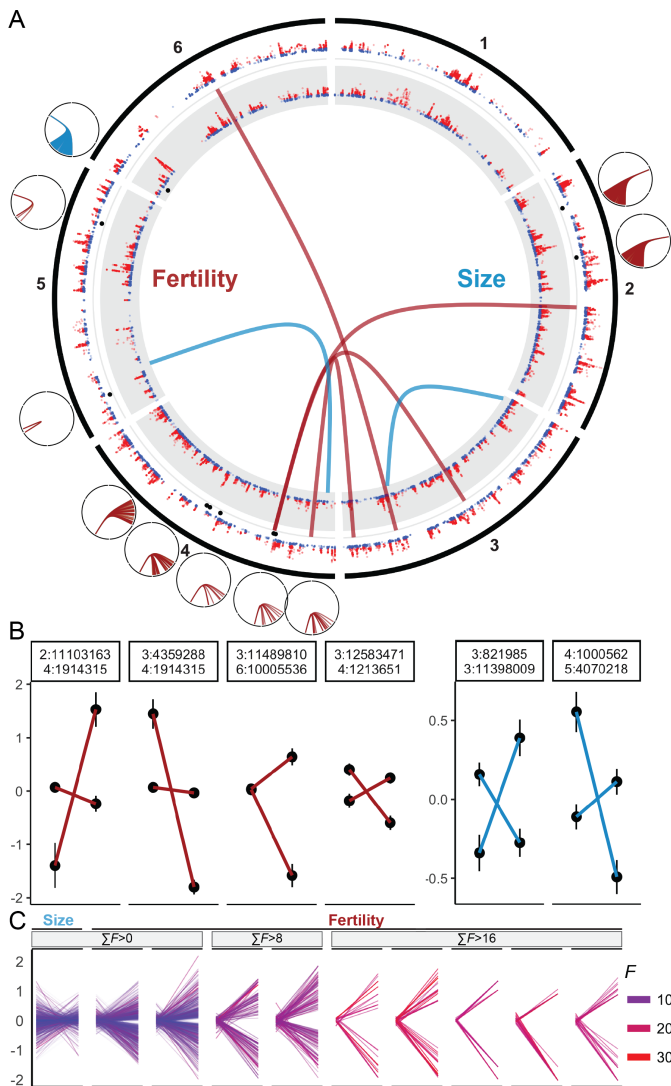


Figure 8 Strong sign epistasis and highly polygenic interactions contribute to trait variance. **A.** The distribution of significant interactions for fertility and size (genetic distance). Pairwise interactions are plotted over 1D GWAS test statistics ($-\log_{10}(p) > 1$) for each trait. Markers with a significant excess of summed interactions for a given chromosome pair are indicated with black points, and the chromosome identities and locations of interacting loci are shown as smaller plots at their approximate positions. 2D sum tests are directed interactions between a single focal marker, and all other markers on one other chromosome, with the sum of interaction scores reaching significance ($\alpha = 0.1$) under a null permutation model. Note interactions between chromosome V:3,145,783 and 16 loci on the right tip of chromosome IV are clustered over a physical interval of 0.44Mb (in weak LD) and appear as a single link at this resolution. **B.** Genotype class trait means (\pm SE) for significant pairs (fertility in red, size in blue). **C.** Genotype class trait means for all individual pairs that contribute to significant summed interactions, at each of the three evaluated F statistic thresholds (interactions significant at $F > 0$ are filtered to $F > 2$ for plotting). Line color and intensity is scaled by F for each constituent interaction. Strong sign epistasis (including weak reciprocal sign epistasis) is the prevalent epistatic mode.

1118 **Conclusions**

1119 We have described the generation, characterization and appli-
 1120 cation of the first multiparental mapping panel for the model
 1121 organism *C. elegans*. Drawing on effectively 260 generations of
 1122 moderate population sizes and predominant outcrossing during
 1123 laboratory culture, full reference-based genome sequencing of
 1124 the 16 inbred wild founders, and dense genotyping of the RILs,
 1125 the CeMEE panel yields gene level mapping resolution for alle-
 1126 les of 5% effect or greater. For traits such as gene expression, for
 1127 which the proportion of variance explained by local variation
 1128 is typically upwards of 20% (e.g., [Brem and Kruglyak \(2005\)](#);
 1129 [Rockman et al. \(2010\)](#); [King et al. \(2014\)](#)), the majority of QTL
 1130 intervals will dissect single genes.

1131 While reference-based genotyping will remain a necessity for
 1132 some time yet, it leaves the contribution of certain classes of
 1133 genetic variation uncertain, and can hamper variant calling due
 1134 to mapping bias and erroneous alignments at copy number vari-
 1135 ants. The genome of only one wild-isolate, the Hawaiian CB4856,
 1136 has been assembled *de novo* to a high standard, revealing exten-
 1137 sive divergence ([Thompson et al. 2015](#)). The ultimate goal of full
 1138 genomes for all founders will yield both better accuracy in calcu-
 1139 lating genetic similarity, and ability to measure the phenotypic
 1140 effects of this recalcitrant variation. Similarly undetermined,
 1141 given RIL genotyping by mostly low coverage sequencing, is
 1142 the extent and fate of novel mutations during experimental evo-
 1143 lution. With a mutation rate of around 1/genome/generation
 1144 for SNPs, and more for multinucleotide mutations and copy
 1145 number variation ([Denver et al. 2004a,b](#); [Seyfert et al. 2008](#); [Den-
 1146 ver et al. 2010](#); [Phillips et al. 2009](#); [Lipinski et al. 2011](#); [Meier
 1147 et al. 2014](#)), the contribution of new mutations to trait variation
 1148 in the RILs may well be non-negligible. Theory suggests that
 1149 fixation of adaptive mutations should not be significant during
 1150 experimental evolution ([Hill 1982](#); [Caballero and Santiago
 1151 1995](#); [Matuszewski et al. 2015](#)), but empirical evidence is mixed
 1152 ([Estes 2004](#); [Estes et al. 2011](#); [Denver et al. 2010](#); [Chelo et al. 2013](#)).
 1153 Both of these factors would erode phenotype prediction accu-
 1154 racy, which, theoretically, should converge on H^2 given perfect
 1155 genotyping of all causal variation and appropriate description
 1156 of genetic covariance ([de los Campos et al. 2015](#)).

1157 The native androdioecious mating system of *C. elegans* and
 1158 the ability to archive strains indefinitely confer significant ad-
 1159 vantages to further use, bestowing almost microbial powers on
 1160 a metazoan model. For one, the preservation of intermediate
 1161 outbred populations means that the CeMEE is readily extensible,
 1162 limited only by effective population sizes. However, RIL panels
 1163 have several potential shortcomings. First, despite inbreeding
 1164 during RIL construction, a nagging concern in use of RIL panels
 1165 is residual heterozygosity ([Barrière et al. 2009](#); [Chelo et al. 2014](#)),
 1166 and the possibility of further evolution of genotypes and phe-
 1167 notypes subsequent to characterization. While heterozygosity
 1168 appears to be at a low level in the CeMEE RILs, on average, it is
 1169 not absent (see [Materials and Methods](#)). Importantly, however,
 1170 given that lines are in stasis the opportunity for segregation dur-
 1171 ing further use is both limited and known. A second concern is
 1172 the possibility of inbreeding depression, particularly for fitness-
 1173 proximal traits. This is a concern for predominantly outcrossing
 1174 organisms ([Barrière et al. 2009](#); [Philip et al. 2011](#); [King et al. 2012](#);
 1175 [Chelo et al. 2014](#)), but it is also applicable to multiparental experi-
 1176 mental evolution of *C. elegans*. As mentioned in the introduction,
 1177 at least during the initial stage of laboratory adaptation, excess
 1178 heterozygosity may have been maintained by epistatic overdom-
 1179 inant selection, and closely linked recessive deleterious alleles

1180 in repulsion could be maintained by balancing selection during
1181 inbreeding (Chelo *et al.* 2013, 2014). Assaying the F_1 progeny of
1182 nested crosses among RILs may be a useful approach to estimate
1183 (or avoid) the effects of inbreeding depression (Long *et al.* 2014).

1184 Using subsets of the CeMEE panel, we outlined the genetics
1185 of two traits associated with fitness. Fertility, as defined here
1186 by the experimental evolution protocol employed, is correlated
1187 with hermaphrodite body size at the time of reproduction (Poul-
1188 let *et al.* 2016). For both traits, and size in particular, additive
1189 genomic heritability based on LD-weighted similarity explained
1190 a significant fraction of H^2 , although heritability estimates were
1191 generally higher with the inclusion of epistatic similarity. This
1192 is consistent with a polygenic architecture with additive effects
1193 below the detection limit, whether solely additive, or due to
1194 weak or opposing effects of multiple interactions. Variance in
1195 fitness-related traits, in particular, may be maintained despite
1196 consistent selection on additive variation through a number of
1197 processes, including stabilizing selection under a stable environ-
1198 ment (Whitlock *et al.* 1995; Wolf *et al.* 2000; Barton and Keightley
1199 2002; Phillips 2008; Hemani *et al.* 2013). Results from variance
1200 decomposition, phenotype prediction and interaction tests are
1201 all consistent with this prediction: phenotypic variance remains
1202 high, and we find support for epistasis for both traits. Notably
1203 for fertility, which is expected to be well aligned with fitness
1204 under the experimental evolution scheme, strong interactions
1205 among four pairs of alleles with weak marginal main effects
1206 jointly explain almost a third of the phenotypic variance. All six
1207 interactions detected for fertility and size are instances of sign
1208 epistasis, where the directional effect of one allele is reversed
1209 in the presence of another. Five of these represent the extreme
1210 form, reciprocal sign epistasis (the reversal is, to some extent at
1211 least, symmetric; Poelwijk *et al.* (2011)). Sign epistasis, in par-
1212 ticular, has important implications for a population's capacity
1213 to adapt, by creating rugged fitness landscapes and constrain-
1214 ing exploration of them (Weinreich *et al.* 2005, 2013), and for
1215 the repeatability of evolution, since the outcome of selection on
1216 the marginal additive effects of interacting alleles will be deter-
1217 mined by their relative frequencies (Wright 1932; Whitlock *et al.*
1218 1995; Phillips *et al.* 2000). Our tests for excess interactions among
1219 individually non-significant marker pairs additionally revealed
1220 a number of cases of highly polygenic epistasis, again, mostly for
1221 fertility. While tests of this type have the unsatisfying property
1222 of leaving the identities of the interacting partners uncertain,
1223 they have the potential to combat the loss of power that comes
1224 with explicit 2-dimensional testing (Crawford *et al.* 2016).

1225 Fertility and body size at reproduction show broad-sense
1226 heritabilities that are relatively high for fitness-proximal traits
1227 (Lynch and Walsh 1998). This high heritability is likely a conse-
1228 quence of novel genetic variation created in the multiparental
1229 cross and realignment of selection to novel laboratory environ-
1230 ments. While all mapping panels are synthetic systems, the mix-
1231 ing of natural variation and experimental evolution represents
1232 a perturbation that may have some parallels, for example, with
1233 that of a simultaneous founder event and environmental change,
1234 which can reveal novel incompatibilities and promote further
1235 differentiation (Cheverud and Routman 1996; Wolf *et al.* 2000).
1236 In this context, it will be useful to determine the directional ef-
1237 fects of epistasis on the genotype-phenotype map during further
1238 evolution, as a function of recombination, a task for which the
1239 CeMEE is well suited. As in other systems such as Arabidop-
1240 sis, where similar resources exist (Weigel 2012) and epistasis for
1241 fitness-related traits has been found (e.g., Malmberg *et al.* (2005);

1242 Simon *et al.* (2008)), it will also be important to begin a com-
1243 prehensive comparison of QTL for fitness traits in the CeMEE
1244 and natural populations – where linked selection coupled with
1245 predominant selfing and meta-population dynamics have gener-
1246 ated limited, structured genetic diversity (Andersen *et al.* 2012;
1247 Rockman *et al.* 2010; Cutter 2015) – and also with mutational
1248 variances obtained in mutation accumulation experiments (Baer
1249 *et al.* 2005; Baer 2008; Joyner-Matos *et al.* 2009). Such compar-
1250 isons have the potential to provide significant insights into how
1251 the distributions of QTL effects and frequencies are shaped in
1252 natural populations.

1253 Acknowledgements

1254 We thank J. Costa, R. Costa, C. Goy, F. Melo, H. Mestre, V. Pereira,
1255 and A. Silva for support with worm handling, sample prepara-
1256 tion, and data acquisition; E. Andersen, M.-A. Félix, P.C. Phillips,
1257 S. Proulx, D. Speed and C. Zheng for helpful discussion.

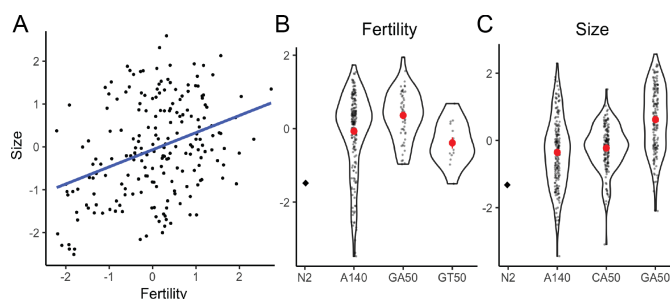
1258 Funding

1259 This work received financial support from the National Insti-
1260 tutes of Health (R01GM089972 and R01GM121828) to MVR,
1261 the Human Frontiers Science Program (RGP0045/2010) to B.S,
1262 M.R. and H.T, and the European Research Council (FP7/2007-
1263 2013/243285) and Agence Nationale de la Recherche (ANR-14-
1264 ACHN-0032-01) to H.T.

1265 Author contributions

1266 CeMEE panel derivation: S.C., B.A., H.T.; sequencing and geno-
1267 typing: A. P.-Q., D.R., I.C. P.A., L.N., M.R.; phenotyping: I.C.,
1268 B.A, A.C.; analysis: L.N., I.C., T.G., A.D, B.S.; manuscript: L.N.,
1269 M.R., H.T.

1270 Supplementary figures



1271 **Figure S1** S1. Trait correlations and evolution. **A.** Fertility and
1272 size are correlated traits (Spearman's $\rho = 0.318$, $p < 5 \times 10^{-6}$
1273 for 202 RILs with data for both traits). **B-C.** Trait distributions
1274 within sub-panels (density plots and mean \pm SE for centered
1275 and scaled model coefficients). The GA50 RILs are signifi-
1276 cantly larger and more fertile than A6140 RILs.

1277 Literature Cited

1272 Abney, M., 2015 Permutation testing in the presence of polygenic
1273 variation. *Genetic epidemiology* **39**: 249–258.
1274 Andersen, E. C., J. S. Bloom, J. P. Gerke, and L. Kruglyak, 2014 A
1275 variant in the neuropeptide receptor *npr-1* is a major determi-
1276 nant of *Caenorhabditis elegans* growth and physiology. *PLOS*
1277 *Genetics* **10**: e1004156.

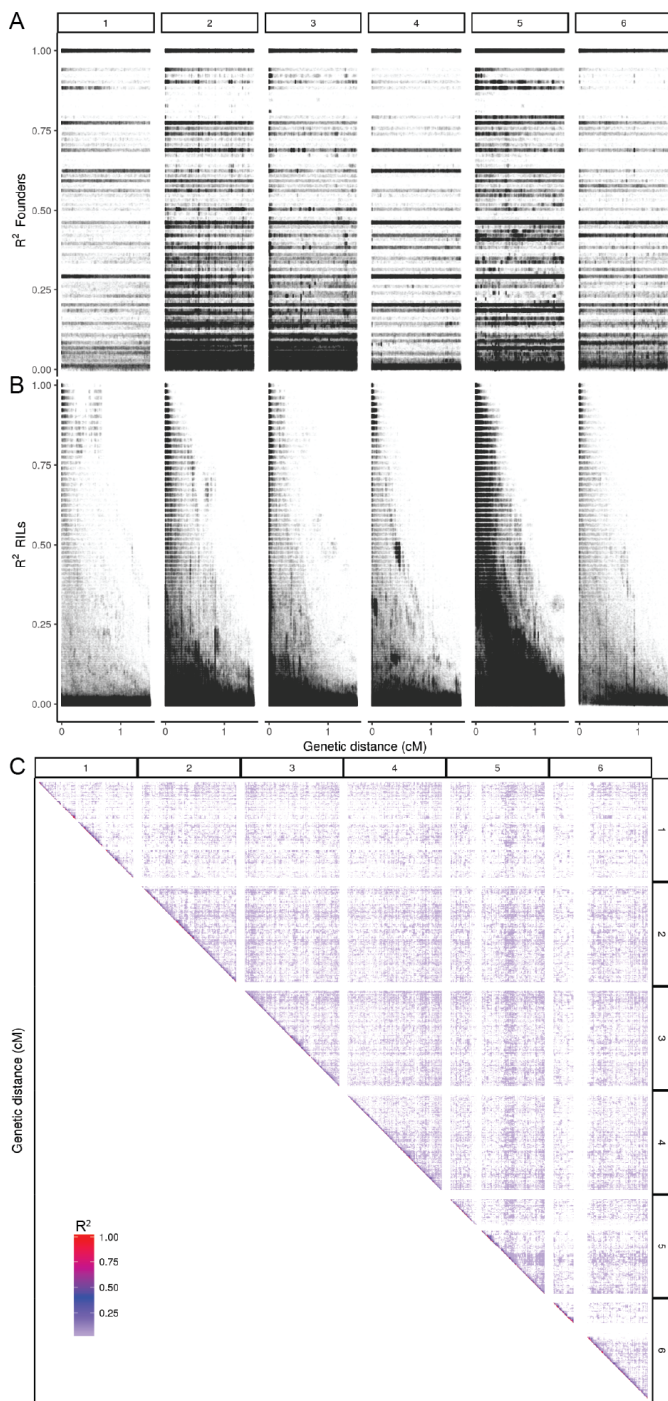


Figure S2 Local linkage disequilibrium in founders **A** and CeMEE RILs **B**, and across RIL genomes (**C**; r^2 thresholded to >0.01).

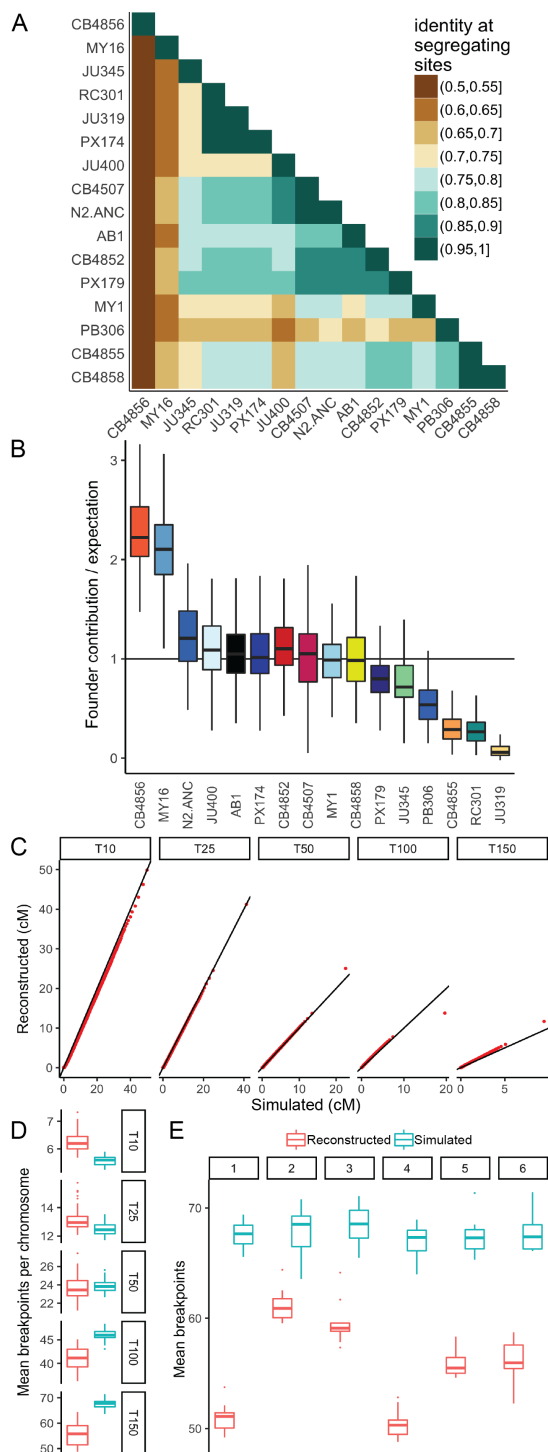


Figure S3 Summary of haplotype reconstruction. **A**. Genetic similarity among founders. **B**. Founder contributions in the CeMEE lines, relative to expectation from reconstruction of simulated recombinant genomes, accounting for bias based on haplotype uniqueness. Boxplots show median (bar), interquartile range (box) and $1.5 \times$ the data range (whiskers). **C**. Haplotype length quantile-quantile plots for known and reconstructed simulations. **D**. The number of breakpoints per chromosome per line across simulation generation. **E**. The number of breakpoints reconstructed by chromosome. Haplotype uniqueness varies across chromosomes: the ability to reconstruct is poorest for chromosomes I and IV.

LITERATURE CITED

LITERATURE CITED

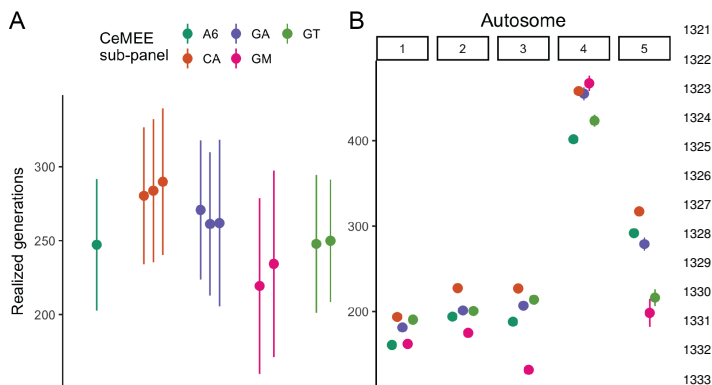


Figure S4 The number of generations of outcrossing for each CeMEE sub-panel (A) and chromosome (B) predicted from the maximum likelihood estimate of realized map expansion (Zheng *et al.* 2014, 2015).

1278 Andersen, E. C., J. P. Gerke, J. A. Shapiro, J. R. Crissman, 1341
 1279 R. Ghosh, J. S. Bloom, M.-A. Félix, and L. Kruglyak, 2012 1342
 1280 Chromosome-scale selective sweeps shape *Caenorhabditis ele-* 1343
 1281 *gans* genomic diversity. *Nature Genetics* **44**: 285–290. 1344
 1282 Andersen, E. C., T. C. Shimko, J. R. Crissman, R. Ghosh, J. S. 1345
 1283 Bloom, H. S. Seidel, J. P. Gerke, and L. Kruglyak, 2015 A 1346
 1284 Powerful New Quantitative Genetics Platform, Combining 1347
 1285 *Caenorhabditis elegans* High-Throughput Fitness Assays with a 1348
 1286 Large Collection of Recombinant Strains. *G3* (Bethesda, Md.) 1349
 1287 **5**: 911–920. 1350
 1288 Anderson, J. L., L. T. Morran, and P. C. Phillips, 2010 Outcrossing 1351
 1289 and the maintenance of males within *C. elegans* populations. 1352
 1290 *The Journal of heredity* **101 Suppl 1**: S62–74. 1353
 1291 Baer, C. F., 2008 Quantifying the Decanalizing Effects of Spon- 1354
 1292 taneous Mutations in Rhabditid Nematodes. *The American* 1355
 1293 *Naturalist* **172**: 272–281. 1356
 1294 Baer, C. F., F. Shaw, C. Steding, M. Baumgartner, A. Hawkins, 1357
 1295 A. Houppert, N. Mason, M. Reed, K. Simonelic, W. Woodard, 1358
 1296 M. Lynch, and W. W. Anderson, 2005 Comparative Evolutionary 1359
 1297 Genetics of Spontaneous Mutations Affecting Fitness in 1360
 1298 Rhabditid Nematodes. *Proceedings of the National Academy* 1361
 1299 *of Sciences of the United States of America* **102**: 5785–5790. 1362
 1300 Baldwin-Brown, J. G., A. D. Long, and K. R. Thornton, 2014 1363
 1301 The power to detect quantitative trait loci using resequenced, 1364
 1302 experimentally evolved populations of diploid, sexual organ- 1365
 1303 isms. *Molecular biology and evolution* **31**: 1040–1055. 1366
 1304 Bandillo, N., C. Raghavan, P. A. Muyco, M. A. L. Sevilla, I. T. 1367
 1305 Lobina, C. J. Dilla-Ermita, C.-W. Tung, S. McCouch, M. Thom- 1368
 1306 son, R. Mauleon, R. K. Singh, G. Gregorio, E. Redoña, and 1369
 1307 H. Leung, 2013 Multi-parent advanced generation inter-cross 1370
 1308 (MAGIC) populations in rice: progress and potential for ge- 1371
 1309 netics research and breeding. *Rice* (New York, N.Y.) **6**: 11. 1372
 1310 Barkoulas, M., J. S. van Zon, J. Milloz, A. van Oudenaarden, 1373
 1311 and M.-A. Félix, 2013 Robustness and Epistasis in the *C. ele-* 1374
 1312 *gans* Vulval Signaling Network Revealed by Pathway Dosage 1375
 1313 Modulation. *Developmental Cell* **24**: 64–75. 1376
 1314 Barrière, A. and M.-A. Félix, 2005 Natural variation and popula- 1377
 1315 tion genetics of *Caenorhabditis elegans*. pp. 1–19. 1378
 1316 Barrière, A. and M.-A. Félix, 2007 Temporal dynamics and link- 1379
 1317 age disequilibrium in natural *Caenorhabditis elegans* popula- 1380
 1318 tions. *Genetics* **176**: 999–1011. 1381
 1319 Barrière, A., S.-P. Yang, E. Pekarek, C. G. Thomas, E. S. Haag, and 1382
 1320 I. Ruvinsky, 2009 Detecting heterozygosity in shotgun genome

assemblies: Lessons from obligately outcrossing nematodes. 1321
 1322 *Genome research* **19**: 470–480. 1323
 1324 Barton, N. H. and P. D. Keightley, 2002 Multifactorial genetics: 1325
 1326 Understanding quantitative genetic variation. *Nature Reviews* 1326
 1327 *Genetics* **3**: 11–21. 1327
 1328 Barton, N. H. and M. Turelli, 1991 Natural and sexual selection 1328
 1329 on many loci. *Genetics* **127**: 229–255. 1329
 1330 Bendesky, A., M. Tsunozaki, M. V. Rockman, L. Kruglyak, and 1330
 1331 C. I. Bargmann, 2011 Catecholamine receptor polymorphisms 1331
 1332 affect decision-making in *C. elegans*. *Nature* **472**: 313–318. 1332
 1333 Bernstein, M. R. and M. V. Rockman, 2016 Fine-Scale Crossover 1333
 1334 Rate Variation on the *Caenorhabditis elegans* X Chromosome. 1334
 1335 *G3* (Bethesda, Md.) **6**: 1767–1776. 1335
 1336 Bloom, J. S., I. Kotenko, M. J. Sadhu, S. Treusch, F. W. Albert, and 1336
 1337 L. Kruglyak, 2015 Genetic interactions contribute less than 1337
 1338 additive effects to quantitative trait variation in yeast. *Nature* 1338
 1339 *communications* **6**: 8712. 1339
 1340 Bonhoeffer, S., C. Chappey, N. T. Parkin, J. M. Whitcomb, and 1340
 1341 C. J. Petropoulos, 2004 Evidence for positive epistasis in HIV-1. 1341
 1342 *Science* (New York, N.Y.) **306**: 1547–1550. 1342
 1343 Bradić, M., J. Costa, and I. M. Chelo, 2011 Genotyping with 1343
 1344 Sequenom. In *Genome-Wide Association Studies and Genomic* 1344
 1345 *Prediction*, pp. 193–210, Humana Press, Totowa, NJ. 1345
 1346 Brem, R. B. and L. Kruglyak, 2005 The landscape of genetic 1346
 1347 complexity across 5,700 gene expression traits in yeast. *Pro-* 1347
 1348 *ceedings of the National Academy of Sciences* **102**: 1572–1577. 1348
 1349 Buckler, E. S., J. B. Holland, P. J. Bradbury, C. B. Acharya, P. J. 1349
 1350 Brown, C. Browne, E. Ersoz, S. Flint-Garcia, A. Garcia, J. C. 1350
 1351 Glaubitz, M. M. Goodman, C. Harjes, K. Guill, D. E. Kroon, 1351
 1352 S. Larsson, N. K. Lepak, H. Li, S. E. Mitchell, G. Pressoir, J. A. 1352
 1353 Peiffer, M. O. Rosas, T. R. Rocheford, M. C. Romay, S. Romero, 1353
 1354 S. Salvo, H. Sanchez Villeda, H. S. da Silva, Q. Sun, F. Tian, 1354
 1355 N. Upadyayula, D. Ware, H. Yates, J. Yu, Z. Zhang, S. Kreso- 1355
 1356 vich, and M. D. McMullen, 2009 The genetic architecture of 1356
 1357 maize flowering time. *Science* (New York, N.Y.) **325**: 714–718. 1357
 1358 Bulik-Sullivan, B. K., P.-R. Loh, H. K. Finucane, S. Ripke, J. Yang, 1358
 1359 N. Patterson, M. J. Daly, A. L. Price, and B. M. Neale, 2015 LD 1359
 1360 Score regression distinguishes confounding from polygenicity 1360
 1361 in genome-wide association studies. *Nature Genetics* **47**: 291– 1361
 1362 295. 1362
 1363 Caballero, A. and E. Santiago, 1995 Response to selection from 1363
 1364 new mutation and effective size of partially inbred popula- 1364
 1365 tions. I. Theoretical results. *Genetical Research* . 1365
 1366 Carlborg, Ö., L. Jacobsson, P. Ahgren, P. Siegel, and L. Andersson, 1366
 1367 2006 Epistasis and the release of genetic variation during long- 1367
 1368 term selection. *Nature Genetics* **38**: 418–420. 1368
 1369 Charlesworth, D. and S. I. Wright, 2001 Breeding systems and 1369
 1370 genome evolution **11**: 685–690. 1370
 1371 Chelo, I. M., S. Carvalho, M. Roque, S. R. Proulx, and H. Teotónio, 1371
 1372 2014 The genetic basis and experimental evolution of inbreed- 1372
 1373 ing depression in *Caenorhabditis elegans*. *Heredity* **112**: 248–254. 1373
 1374 Chelo, I. M., J. Nédli, I. Gordo, and H. Teotónio, 2013 An exper- 1374
 1375 imental test on the probability of extinction of new genetic 1375
 1376 variants. *Nature communications* **4**: 2417. 1376
 1377 Chelo, I. M. and H. Teotónio, 2013 The opportunity for balancing 1377
 1378 selection in experimental populations of *Caenorhabditis elegans*. 1378
 1379 *Evolution* **67**: 142–156. 1379
 1380 Cheverud, J. M. and E. J. Routman, 1995 Epistasis and its contri- 1380
 1381 bution to genetic variance components. *Genetics* . 1381
 1382 Cheverud, J. M. and E. J. Routman, 1996 Epistasis as a Source 1382
 of Increased Additive Genetic Variance at Population Bottle-
 necks. *Evolution* **50**: 1042.

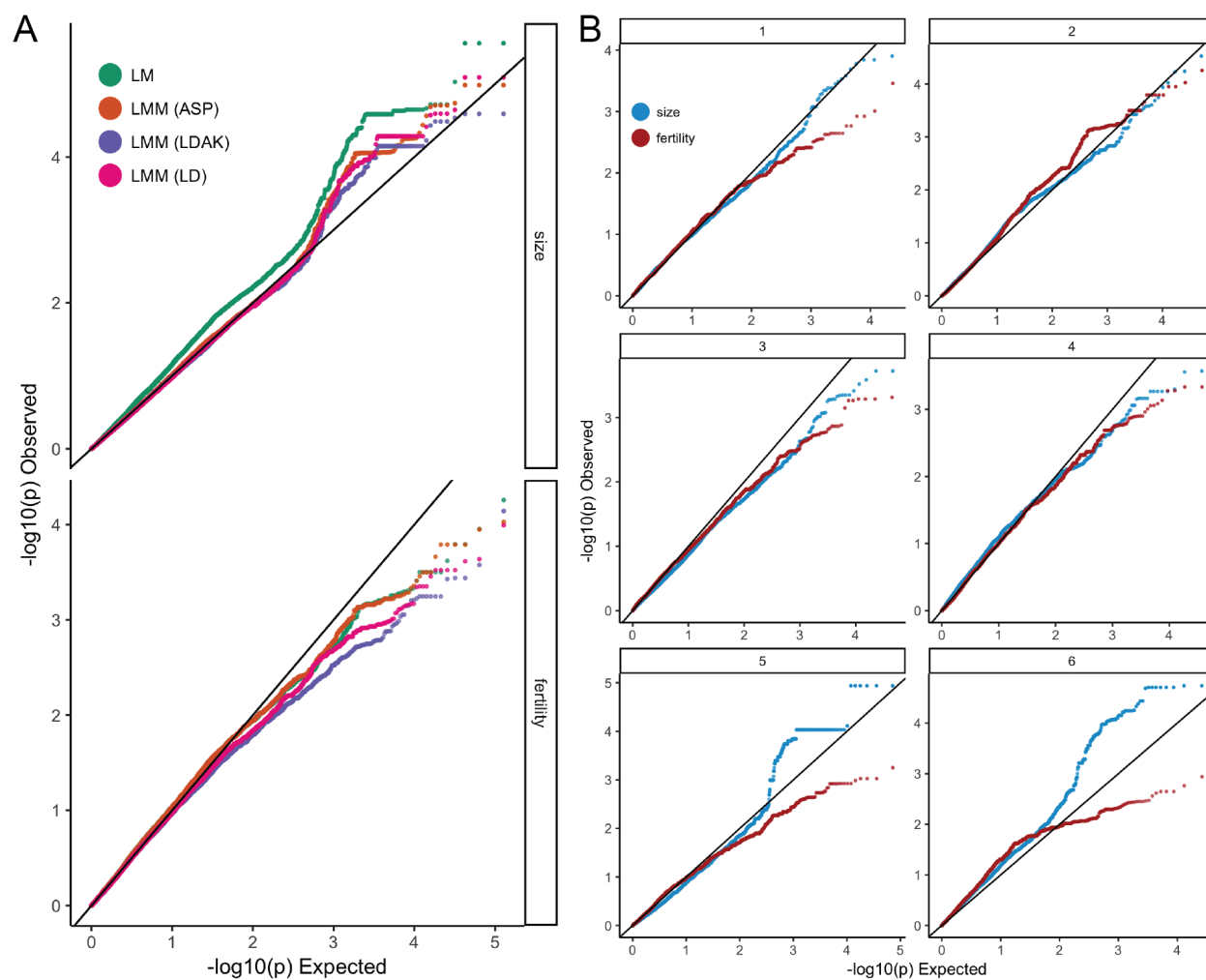


Figure S5 p -value quantile-quantile plots genome-wide (A), comparing the effects of relatedness corrections (where LM is linear model; LMM (ASP) is linear mixed model with relatedness based on allele sharing probability (all markers, equally weighted); LMM (LDAK) is the best performing LD-weighted similarity for each trait; LMM (LD) is based on markers pruned by local LD, but unweighted), and by chromosome (B), for the best LD-weighted similarity for each trait. While strong, spurious inflation is seen for size without polygenic correction (A), this is not seen for fertility, likely due the greater heterogeneity of trait values among sub-panels for size. Notably, deflation is seen for fertility for all models, although LD weighting introduces the strongest penalty, which may indicate a relationship between low LD and causal variation for this trait.

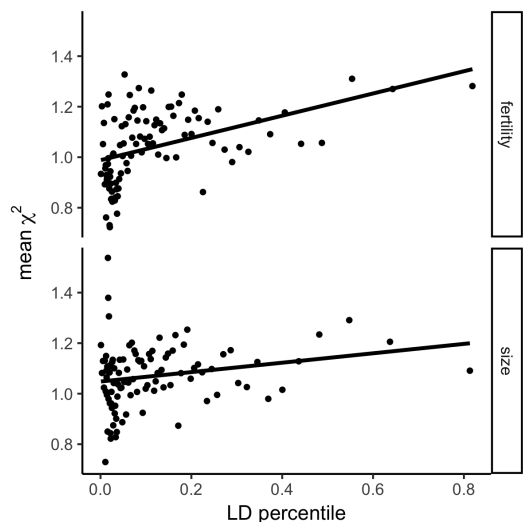


Figure S6 Fitness-proximal traits are polygenic. Regression of association statistics (mean value of χ^2 percentiles) on marker LD weightings (mean of w percentiles, [Speed et al. \(2012\)](#)) for fertility and size (after [Bulik-Sullivan et al. \(2015\)](#)). While there is a significant positive relationship between trait association and the amount of variation tagged by markers, fertility shows much stronger evidence of polygenicity (slope=0.44, $p = 2.7 \times 10^{-6}$, versus slope=0.19, $p = 0.029$ for size).

1383 Chirgwin, E., D. J. Marshall, C. M. Sgrò, and K. Monro, 2016
 1384 The other 96%: Can neglected sources of fitness variation offer
 1385 new insights into adaptation to global change? *Evolutionary*
 1386 *Applications* **10**: 267–275.
 1387 Churchill, G. A., D. C. Airey, H. Allayee, J. M. Angel, A. D. Attie,
 1388 J. Beatty, W. D. Beavis, J. K. Belknap, B. Bennett, W. Berret-
 1389 tini, A. Bleich, M. Bogue, K. W. Broman, K. J. Buck, E. Buck-
 1390 ler, M. Burmeister, E. J. Chesler, J. M. Cheverud, S. Clapcote,
 1391 M. N. Cook, R. D. Cox, J. C. Crabbe, W. E. Crusio, A. Dar-
 1392 vasi, C. F. Deschepper, R. W. Doerge, C. R. Farber, J. Forejt,
 1393 D. Gaile, S. J. Garlow, H. Geiger, H. Gershenfeld, T. Gordon,
 1394 J. Gu, W. Gu, G. de Haan, N. L. Hayes, C. Heller, H. Him-
 1395 melbauer, R. Hitzemann, K. Hunter, H.-C. Hsu, F. A. Iraqi,
 1396 B. Ivandic, H. J. Jacob, R. C. Jansen, K. J. Jepsen, D. K. John-
 1397 son, T. E. Johnson, G. Kempermann, C. Kendziorski, M. Kotb,
 1398 R. F. Kooy, B. Llamas, F. Lammert, J.-M. Lassalle, P. R. Lowen-
 1399 stein, L. Lu, A. Lusi, K. F. Manly, R. Marcucio, D. Matthews,
 1400 J. F. Medrano, D. R. Miller, G. Mittleman, B. A. Mock, J. S.
 1401 Mogil, X. Montagutelli, G. Morahan, D. G. Morris, R. Mott,
 1402 J. H. Nadeau, H. Nagase, R. S. Nowakowski, B. F. O’Hara,
 1403 A. V. Osadchuk, G. P. Page, B. Paigen, K. Paigen, A. A. Palmer,
 1404 H.-J. Pan, L. Peltonen-Palotie, J. Peirce, D. Pomp, M. Pravenec,
 1405 D. R. Prows, Z. Qi, R. H. Reeves, J. Roder, G. D. Rosen, E. E.
 1406 Schadt, L. C. Schalkwyk, Z. Seltzer, K. Shimomura, S. Shou,
 1407 M. J. Sillanpää, L. D. Siracusa, H.-W. Snoeck, J. L. Spearow,
 1408 K. Svenson, L. M. Tarantino, D. Threadgill, L. A. Toth, W. Val-
 1409 dar, F. P.-M. de Villena, C. Warden, S. Whatley, R. W. Williams,
 1410 T. Wiltshire, N. Yi, D. Zhang, M. Zhang, and F. Zou, 2004 The
 1411 Collaborative Cross, a community resource for the genetic
 1412 analysis of complex traits. *Nature Genetics* **36**: 1133–1137.
 1413 Cook, D. E., S. Zdraljevic, J. P. Roberts, and E. C. Andersen, 2017
 1414 CeNDR, the *Caenorhabditis elegans* natural diversity resource.
 1415 *Nucleic acids research* **45**: D650–D657.
 1416 Cook, D. E., S. Zdraljevic, R. E. Tanny, B. Seo, D. D. Riccardi,

1417 L. M. Noble, M. V. Rockman, M. J. Alkema, C. Braendle, J. E.
 1418 Kammenga, J. Wang, L. Kruglyak, M.-A. Félix, J. Lee, and
 1419 E. C. Andersen, 2016 The Genetic Basis of Natural Variation in
 1420 *Caenorhabditis elegans* Telomere Length. *Genetics* **204**: 371–383.
 1421 Corsi, A. K., B. Wightman, and M. Chalfie, 2015 A Transpa-
 1422 rent Window into Biology: A Primer on *Caenorhabditis elegans*.
 1423 *Genetics* **200**: 387–407.
 1424 Crawford, L., S. Mukherjee, and X. Zhou, 2016 Detecting Epis-
 1425 tasis in Genome-wide Association Studies with the Marginal
 1426 EPIstasis Test. *bioRxiv* p. 066985.
 1427 Cutter, A. D., 2004 Sperm-limited fecundity in nematodes: how
 1428 many sperm are enough? *Evolution* **58**: 651–655.
 1429 Cutter, A. D., 2006 Nucleotide polymorphism and linkage dise-
 1430 quilibrium in wild populations of the partial selfer *Caenorhab-*
 1431 *ditis elegans*. *Genetics* **172**: 171–184.
 1432 Cutter, A. D., 2015 *Caenorhabditis* evolution in the wild. *BioEs-*
 1433 *says : news and reviews in molecular, cellular and develop-*
 1434 *mental biology* **37**: 983–995.
 1435 Cutter, A. D., A. Dey, and R. L. Murray, 2009 Evolution of the
 1436 *Caenorhabditis elegans* genome .
 1437 de Bono, M. and C. I. Bargmann, 1998 Natural variation in a
 1438 neuropeptide Y receptor homolog modifies social behavior
 1439 and food response in *C. elegans*. *Cell* **94**: 679–689.
 1440 de los Campos, G., D. Sorensen, and D. Gianola, 2015 Genomic
 1441 Heritability: What Is It? *PLOS Genetics* **11**: e1005048.
 1442 de Visser, J. A. G. M., S.-C. Park, and J. Krug, 2009 Exploring the
 1443 effect of sex on empirical fitness landscapes. *The American*
 1444 *Naturalist* **174 Suppl 1**: S15–30.
 1445 Denver, D. R., D. K. Howe, L. J. Wilhelm, C. A. Palmer, J. L.
 1446 Anderson, K. C. Stein, P. C. Phillips, and S. Estes, 2010 Selec-
 1447 tive sweeps and parallel mutation in the adaptive recovery
 1448 from deleterious mutation in *Caenorhabditis elegans*. *Genome*
 1449 *research* **20**: 1663–1671.
 1450 Denver, D. R., K. Morris, A. Kewalramani, K. E. Harris, A. Chow,
 1451 S. Estes, M. Lynch, and W. K. Thomas, 2004a Abundance, dis-
 1452 tribution, and mutation rates of homopolymeric nucleotide
 1453 runs in the genome of *Caenorhabditis elegans*. *Journal of molec-*
 1454 *ular evolution* **58**: 584–595.
 1455 Denver, D. R., K. Morris, M. Lynch, and W. K. Thomas, 2004b
 1456 High mutation rate and predominance of insertions in the
 1457 *Caenorhabditis elegans* nuclear genome. *Nature* **430**: 679–682.
 1458 Diaz, S. A. and M. Viney, 2014 Genotypic-specific variance in
 1459 *Caenorhabditis elegans* lifetime fecundity. *Ecology and Evolu-*
 1460 *tion* **4**: 2058–2069.
 1461 Dohm, M. R., 2002 Repeatability Estimates Do Not Always Set an
 1462 Upper Limit to Heritability. *Functional Ecology* **16**: 273–280.
 1463 Dolgin, E. S., B. Charlesworth, S. E. Baird, and A. D. Cutter, 2007
 1464 Inbreeding and Outbreeding Depression in *Caenorhabditis*
 1465 *Nematodes*. *Evolution* **61**: 1339–1352.
 1466 Doroszuk, A., L. B. Snoek, E. Fradin, J. Riksen, and J. Kammenga,
 1467 2009 A genome-wide library of CB4856/N2 introgression lines
 1468 of *Caenorhabditis elegans*. *Nucleic acids research* **37**: e110–e110.
 1469 Duveau, F. and M.-A. Félix, 2012 Role of pleiotropy in the evolu-
 1470 tion of a cryptic developmental variation in *Caenorhabditis*
 1471 *elegans*. *PLoS biology* **10**: e1001230.
 1472 Estes, S., 2004 Mutation Accumulation in Populations of Vary-
 1473 ing Size: The Distribution of Mutational Effects for Fitness
 1474 Correlates in *Caenorhabditis elegans*. *Genetics* **166**: 1269–1279.
 1475 Estes, S., 2005 Spontaneous Mutational Correlations for
 1476 Life-History, Morphological and Behavioral Characters in
 1477 *Caenorhabditis elegans*. *Genetics* **170**: 645–653.
 1478 Estes, S. and M. Lynch, 2003 Rapid Fitness Recovery in Muta-

LITERATURE CITED

LITERATURE CITED

- tionally Degraded Lines of *Caenorhabditis elegans*. *Evolution* **57**: 1022–1030.
- Estes, S., P. C. Phillips, and D. R. Denver, 2011 FITNESS RECOVERY AND COMPENSATORY EVOLUTION IN NATURAL MUTANT LINES OF *C. ELEGANS*. *Evolution* **65**: 2335–2344.
- Etienne, V., E. C. Andersen, J. M. Ponciano, D. Blanton, A. Cadavid, J. Joyner-Matos, C. Matsuba, B. Tabman, and C. F. Baer, 2015 The red death meets the abdominal bristle: polygenic mutation for susceptibility to a bacterial pathogen in *Caenorhabditis elegans*. *Evolution* **69**: 508–519.
- Falconer, D. S., 1981 *Introduction to quantitative genetics*. Longman Publishing Group.
- Farhadifar, R., J. M. Ponciano, E. C. Andersen, D. J. Needleman, and C. F. Baer, 2016 Mutation Is a Sufficient and Robust Predictor of Genetic Variation for Mitotic Spindle Traits in *Caenorhabditis elegans*. *Genetics* **203**: 1859–1870.
- Félix, M.-A. and M. Barkoulas, 2015 Pervasive robustness in biological systems. *Nature Reviews Genetics* **16**: 483–496.
- Fisher, R. A., 1930 *The Genetical Theory of Natural Selection*. A Complete Variorum Edition, Oxford University Press.
- Forsberg, S. K. G., J. S. Bloom, M. J. Sadhu, L. Kruglyak, and Ö. Carlborg, 2017 Accounting for genetic interactions improves modeling of individual quantitative trait phenotypes in yeast. *Nature Genetics* **139**: 1455.
- Gaertner, B. E., M. D. Parmenter, M. V. Rockman, L. Kruglyak, and P. C. Phillips, 2012 More than the sum of its parts: a complex epistatic network underlies natural variation in thermal preference behavior in *Caenorhabditis elegans*. *Genetics* **192**: 1533–1542.
- Galton, F., 1886 Regression Towards Mediocrity in Hereditary Stature. *The Journal of the Anthropological Institute of Great Britain and Ireland* **15**: 246.
- Gems, D. and D. L. Riddle, 2000 Defining wild-type life span in *Caenorhabditis elegans*. *The journals of gerontology. Series A, Biological sciences and medical sciences* **55**: B215–9.
- Ghosh, R., E. C. Andersen, J. A. Shapiro, J. P. Gerke, and L. Kruglyak, 2012 Natural variation in a chloride channel subunit confers avermectin resistance in *C. elegans*. *Science (New York, N.Y.)* **335**: 574–578.
- Gimond, C., R. Jovelin, S. Han, C. Ferrari, A. D. Cutter, and C. Braendle, 2013 Outbreeding depression with low genetic variation in selfing *Caenorhabditis nematodes*. *Evolution* **67**: 3087–3101.
- Gloria-Soria, A. and R. B. R. Azevedo, 2008 *npr-1* Regulates foraging and dispersal strategies in *Caenorhabditis elegans*. *Current biology : CB* **18**: 1694–1699.
- Goddard, M. E., K. E. Kemper, I. M. MacLeod, A. J. Chamberlain, and B. J. Hayes, 2016 Genetics of complex traits: prediction of phenotype, identification of causal polymorphisms and genetic architecture. *Proc. R. Soc. B* **283**: 20160569.
- Gray, J. C. and A. D. Cutter, 2014 Mainstreaming *Caenorhabditis elegans* in experimental evolution. *Proceedings. Biological sciences* **281**: 20133055–20133055.
- Greene, J. S., M. Brown, M. Dobosiewicz, I. G. Ishida, E. Z. Macosko, X. Zhang, R. A. Butcher, D. J. Cline, P. T. McGrath, and C. I. Bargmann, 2016 Balancing selection shapes density-dependent foraging behaviour. *Nature* **539**: 254–258.
- Gruber, J. D., K. Vogel, G. Kalay, and P. J. Wittkopp, 2012 Contrasting properties of gene-specific regulatory, coding, and copy number mutations in *Saccharomyces cerevisiae*: frequency, effects, and dominance. *PLOS Genetics* **8**: e1002497.
- Gutteling, E. W., A. Doroszuk, J. A. G. Riksen, Z. Prokop, J. Reszka, and J. E. Kammenga, 2007 Environmental influence on the genetic correlations between life-history traits in *Caenorhabditis elegans*. *Heredity* **98**: 206–213.
- Halligan, D. L. and P. D. Keightley, 2009 Spontaneous Mutation Accumulation Studies in Evolutionary Genetics. *Annual Review of Ecology, Evolution, and Systematics* **40**: 151–172.
- Hansen, T. F., 2013 WHY EPISTASIS IS IMPORTANT FOR SELECTION AND ADAPTATION **67**: 3501–3511.
- Hayes, J. P. and S. H. Jenkins, 1997 Individual Variation in Mammals. *Journal of Mammalogy* **78**: 274–293.
- Hemani, G., S. Knott, and C. Haley, 2013 An Evolutionary Perspective on Epistasis and the Missing Heritability. *PLOS Genetics* **9**: e1003295.
- Henderson, C. R., 1975 Best Linear Unbiased Estimation and Prediction under a Selection Model **31**: 423.
- Henderson, C. R., 1985 Best Linear Unbiased Prediction of Non-additive Genetic Merits in Noninbred Populations. *Journal of animal science* **60**: 111–117.
- Hill, W. G., 1982 Rates of change in quantitative traits from fixation of new mutations. *Proceedings of the National Academy of Sciences* **79**: 142–145.
- Hill, W. G., M. E. Goddard, and P. M. Visscher, 2008 Data and Theory Point to Mainly Additive Genetic Variance for Complex Traits **4**: e1000008.
- Hirsh, D., D. Oppenheim, and M. Klass, 1976 Development of the reproductive system of *Caenorhabditis elegans*. *Developmental biology* **49**: 200–219.
- Huang, A., S. Xu, and X. Cai, 2014 Whole-genome quantitative trait locus mapping reveals major role of epistasis on yield of rice. *PloS one* **9**: e87330.
- Huang, B. E., A. W. George, K. L. Forrest, A. Kilian, M. J. Hayden, M. K. Morell, and C. R. Cavanagh, 2012 A multiparent advanced generation inter-cross population for genetic analysis in wheat. *Plant biotechnology journal* **10**: 826–839.
- Jiang, Y. and J. C. Reif, 2015 Modeling Epistasis in Genomic Selection. *Genetics* **201**: 759–768.
- Jombart, T., 2008 adegenet: a R package for the multivariate analysis of genetic markers. *Bioinformatics (Oxford, England)* **24**: 1403–1405.
- Jombart, T., S. Devillard, and F. Balloux, 2010 Discriminant analysis of principal components: a new method for the analysis of genetically structured populations. *BMC genetics* **11**: 94.
- Joyner-Matos, J., A. Upadhyay, M. P. Salomon, V. Grigaltchik, and C. F. Baer, 2009 Genetic (Co)variation for life span in rhabditid nematodes: role of mutation, selection, and history. *The journals of gerontology. Series A, Biological sciences and medical sciences* **64**: 1134–1145.
- Kamran-Disfani, A. and A. F. Agrawal, 2014 Selfing, adaptation and background selection in finite populations. *Journal of evolutionary biology* **27**: 1360–1371.
- Kaur, T. and M. V. Rockman, 2014 Crossover heterogeneity in the absence of hotspots in *Caenorhabditis elegans*. *Genetics* **196**: 137–148.
- King, E. G., S. J. Macdonald, and A. D. Long, 2012 Properties and power of the *Drosophila* Synthetic Population Resource for the routine dissection of complex traits. *Genetics* **191**: 935–949.
- King, E. G., B. J. Sanderson, C. L. McNeil, A. D. Long, and S. J. Macdonald, 2014 Genetic dissection of the *Drosophila melanogaster* female head transcriptome reveals widespread allelic heterogeneity. *PLOS Genetics* **10**: e1004322.
- Knight, C. G., R. B. Azevedo, and A. M. Leroi, 2001 Testing life-history pleiotropy in *Caenorhabditis elegans*. **55**: 1795–1804.

LITERATURE CITED

LITERATURE CITED

- 1603 Kover, P. X., W. Valdar, J. Trakalo, N. Scarcelli, I. M. Ehrenreich, 1665
1604 M. D. Purugganan, C. Durrant, and R. Mott, 2009 A Multipar- 1666
1605 ent Advanced Generation Inter-Cross to Fine-Map Quantita- 1667
1606 tive Traits in *Arabidopsis thaliana*. *PLOS Genetics* 5: e1000551. 1668
1607 Lessells, C. M. and P. T. Boag, 1987 Unrepeatable Repeatabilities: 1669
1608 A Common Mistake. *The Auk* 104: 116–121. 1670
1609 Li, H. and R. Durbin, 2010 Fast and accurate long-read align- 1671
1610 ment with Burrows-Wheeler transform. *Bioinformatics* (Ox- 1672
1611 ford, England) 26: 589–595. 1673
1612 Lipinski, K. J., J. C. Farslow, K. A. Fitzpatrick, M. Lynch, V. Katju, 1674
1613 and U. Bergthorsson, 2011 High Spontaneous Rate of Gene 1675
1614 Duplication in *Caenorhabditis elegans*. *Current Biology* 21: 306– 1676
1615 310. 1677
1616 Long, A. D., S. J. Macdonald, and E. G. King, 2014 Dissecting 1678
1617 complex traits using the *Drosophila* Synthetic Population Re- 1679
1618 source. *Trends in genetics : TIG* 30: 488–495. 1680
1619 Lynch, M. and B. Walsh, 1998 *Genetics and Analysis of Quantitative* 1681
1620 *Traits*. Sinauer Associates Incorporated. 1682
1621 Macdonald, S. J. and A. D. Long, 2007 Joint estimates of quanti- 1683
1622 tative trait locus effect and frequency using synthetic recom- 1684
1623 binant populations of *Drosophila melanogaster*. *Genetics* 176: 1685
1624 1261–1281. 1686
1625 Mackay, I. J., P. Bansept-Basler, T. Barber, A. R. Bentley, J. Cock- 1687
1626 ram, N. Gosman, A. J. Greenland, R. Horsnell, R. Howells, 1688
1627 D. M. O’Sullivan, G. A. Rose, and P. J. Howell, 2014 An eight- 1689
1628 parent multiparent advanced generation inter-cross popula- 1690
1629 tion for winter-sown wheat: creation, properties, and valida- 1691
1630 tion. *G3* (Bethesda, Md.) 4: 1603–1610. 1692
1631 Malmberg, R. L., S. Held, A. Waits, and R. Mauricio, 2005 Epista- 1693
1632 sis for fitness-related quantitative traits in *Arabidopsis thaliana* 1694
1633 grown in the field and in the greenhouse. *Genetics* 171: 2013– 1695
1634 2027. 1696
1635 Manolio, T. A., F. S. Collins, N. J. Cox, D. B. Goldstein, L. A. 1697
1636 Hindorf, D. J. Hunter, M. I. McCarthy, E. M. Ramos, L. R. 1698
1637 Cardon, A. Chakravarti, J. H. Cho, A. E. Guttmacher, A. Kong, 1699
1638 L. Kruglyak, E. Mardis, C. N. Rotimi, M. Slatkin, D. Valle, A. S. 1700
1639 Whittemore, M. Boehnke, A. G. Clark, E. E. Eichler, G. Gibson, 1701
1640 J. L. Haines, T. F. C. Mackay, S. A. McCarroll, and P. M. Viss- 1702
1641 cher, 2009 Finding the missing heritability of complex diseases. 1703
1642 *461: 747–753*. 1704
1643 Marouli, E., M. Graff, C. Medina-Gomez, K. S. Lo, A. R. Wood, 1705
1644 T. R. Kjaer, R. S. Fine, Y. Lu, C. Schurmann, H. M. Highland, 1706
1645 S. Rueger, G. Thorleifsson, A. E. Justice, D. Lamparter, K. E. 1707
1646 Stirrups, V. Turcot, K. L. Young, T. W. Winkler, T. Esko, T. Ka- 1708
1647 raderi, A. E. Locke, N. G. D. Masca, M. C. Y. Ng, P. Mudgal, 1709
1648 M. A. Rivas, S. Vedantam, A. Mahajan, X. Guo, G. Abeca- 1710
1649 sis, K. K. Aben, L. S. Adair, D. S. Alam, E. Albrecht, K. H. 1711
1650 Allin, M. Allison, P. Amouyel, E. V. Appel, D. Arveiler, 1712
1651 F. W. Asselbergs, P. L. Auer, B. Balkau, B. Banas, L. E. Bang, 1713
1652 M. Benn, S. Bergmann, L. F. Bielak, M. Blüher, H. Boeing, 1714
1653 E. Boerwinkle, C. A. Böger, L. L. Bonnycastle, J. Bork-Jensen, 1715
1654 M. L. Bots, E. P. Bottinger, D. W. Bowden, I. Brandslund, 1716
1655 G. Breen, M. H. Brilliant, L. Broer, A. A. Burt, A. S. Butter- 1717
1656 worth, D. J. Carey, M. J. Caulfield, J. C. Chambers, D. I. Chas- 1718
1657 man, Y.-D. I. Chen, R. Chowdhury, C. Christensen, A. Y. Chu, 1719
1658 M. Cocca, F. S. Collins, J. P. Cook, J. Corley, J. C. Galbany, 1720
1659 A. J. Cox, G. Cuellar-Partida, J. Danesh, G. Davies, P. I. W. 1721
1660 de Bakker, G. J. de Borst, S. de Denu, M. C. H. de Groot, 1722
1661 R. de Mutsert, I. J. Deary, G. Dedoussis, E. W. Demerath, A. I. 1723
1662 den Hollander, J. G. Dennis, E. Di Angelantonio, F. Drenos, 1724
1663 M. Du, A. M. Dunning, D. F. Easton, T. Ebeling, T. L. Ed- 1725
1664 wards, P. T. Ellinor, P. Elliott, E. Evangelou, A.-E. Farmaki, 1726
J. D. Faul, M. F. Feitosa, S. Feng, E. Ferrannini, M. M. Fer-
rario, J. Ferrieres, J. C. Florez, I. Ford, M. Fornage, P. W.
Franks, R. Frikke-Schmidt, T. E. Galesloot, W. Gan, I. Gandin,
P. Gasparini, V. Giedraitis, A. Giri, G. Girotto, S. D. Gor-
don, P. Gordon-Larsen, M. Gorski, N. Grarup, M. L. Grove,
V. Gudnason, S. Gustafsson, T. Hansen, K. M. Harris, T. B.
Harris, A. T. Hattersley, C. Hayward, L. He, I. M. Heid,
K. Heikkilä, Ø. Helgeland, J. Hernesniemi, A. W. Hewitt,
L. J. Hocking, M. Hollensted, O. L. Holmen, G. K. Hovingh,
J. M. M. Howson, C. B. Hoyng, P. L. Huang, K. Hveem, M. A.
Ikram, E. Ingelsson, A. U. Jackson, J.-H. Jansson, G. P. Jarvik,
G. B. Jensen, M. A. Jhun, Y. Jia, X. Jiang, S. Johansson, M. E.
Jørgensen, T. Jørgensen, P. Jousilahti, J. W. Jukema, B. Ka-
hali, R. S. Kahn, M. Kähönen, P. R. Kamstrup, S. Kanoni,
J. Kaprio, M. Karaleftheri, S. L. R. Kardina, F. Karpe, F. Kee,
R. Keeman, L. A. Kiemeny, H. Kitajima, K. B. Kluijvers,
T. Kocher, P. Komulainen, J. Kontto, J. S. Kooner, C. Kooper-
berg, P. Kovacs, J. Kriebel, H. Kuivaniemi, S. Küry, J. Kuusisto,
M. La Bianca, M. Laakso, T. A. Lakka, E. M. Lange, L. A.
Lange, C. D. Langefeld, C. Tangenberger, E. B. Larson, I.-T. Lee,
T. Lehtimäki, C. E. Lewis, H. Li, J. Li, R. Li-Gao, H. Lin, L.-A.
Lin, X. Lin, L. Lind, J. Lindström, A. Linneberg, Y. Liu, Y. Liu,
A. Lophatananon, J. Luan, S. A. Lubitz, L.-P. Lyytikäinen,
D. A. Mackey, P. A. F. Madden, A. K. Manning, S. Männistö,
G. Marenne, J. Marten, N. G. Martin, A. L. Mazul, K. Meidtner,
A. Metspalu, P. Mitchell, K. L. Mohlke, D. O. Mook-Kanamori,
A. Morgan, A. D. Morris, A. P. Morris, M. Müller-Nurasyid,
P. B. Munroe, M. A. Nalls, and M. Nauck, 2017 Rare and low-
frequency coding variants alter human adult height. *Nature*
542: 186–190.
Masri, L., R. D. Schulte, N. Timmermeyer, S. Thanisch, L. L.
Crummenerl, G. Jansen, N. K. Michiels, and H. Schulenburg,
2013 Sex differences in host defence interfere with parasite-
mediated selection for outcrossing during host-parasite coevo-
lution. *Ecology letters* 16: 461–468.
Matuszewski, S., J. Hermisson, and M. Kopp, 2015 Catch Me if
You Can: Adaptation from Standing Genetic Variation to a
Moving Phenotypic Optimum. *Genetics* 200: 1255–1274.
Maupas, E., 1900 Modes et formes de reproduction des nema-
todes. *Archives de zoologie expérimentale et générale* pp.
463–624.
McGrath, P. T., M. V. Rockman, M. Zimmer, H. Jang, E. Z. Ma-
cosko, L. Kruglyak, and C. I. Bargmann, 2009 Quantitative
mapping of a digenic behavioral trait implicates globin varia-
tion in *C. elegans* sensory behaviors. *Neuron* 61: 692–699.
McKenna, A., M. Hanna, E. Banks, A. Sivachenko, K. Cibulskis,
A. Kernytzky, K. Garimella, D. Altshuler, S. Gabriel, M. Daly,
and M. A. DePristo, 2010 The Genome Analysis Toolkit: a
MapReduce framework for analyzing next-generation DNA
sequencing data. *Genome research* 20: 1297–1303.
McMullen, M. D., S. Kresovich, H. S. Villeda, P. Bradbury, H. Li,
Q. Sun, S. Flint-Garcia, J. Thornsberry, C. Acharya, C. Bottoms,
P. Brown, C. Browne, M. Eller, K. Guill, C. Harjes, D. Kroon,
N. Lepak, S. E. Mitchell, B. Peterson, G. Pressoir, S. Romero,
M. O. Rosas, S. Salvo, H. Yates, M. Hanson, E. Jones, S. Smith,
J. C. Glaubitz, p. M. p. Goodman, D. Ware, J. B. Holland, and
E. S. Buckler, 2009 Genetic Properties of the Maize Nested
Association Mapping Population. *Science* (New York, N.Y.)
325: 737–740.
Meier, B., S. L. Cooke, J. Weiss, A. P. Bailly, L. B. Alexandrov,
J. Marshall, K. Raine, M. Maddison, E. Anderson, M. R. Strat-
ton, A. Gartner, and P. J. Campbell, 2014 *C. elegans* whole-

LITERATURE CITED

LITERATURE CITED

- 1727 genome sequencing reveals mutational signatures related to 1789
1728 carcinogens and DNA repair deficiency. *Genome research* **24**: 1790
1729 1624–1636. 1791
- 1730 Meuwissen, T. and M. Goddard, 2010 Accurate prediction of 1792
1731 genetic values for complex traits by whole-genome resequenc- 1793
1732 ing. *Genetics* **185**: 623–631. 1794
- 1733 Meuwissen, T. H., B. J. Hayes, and M. E. Goddard, 2001 Predic- 1795
1734 tion of total genetic value using genome-wide dense marker 1796
1735 maps. *Genetics* **157**: 1819–1829. 1797
- 1736 Monnahan, P. J. and J. K. Kelly, 2015a Epistasis Is a Major Deter- 1798
1737 minant of the Additive Genetic Variance in *Mimulus guttatus*. 1799
1738 *PLOS Genetics* **11**: e1005201. 1800
- 1739 Monnahan, P. J. and J. K. Kelly, 2015b Naturally segregating loci 1801
1740 exhibit epistasis for fitness. *Biology Letters* **11**: 20150498. 1802
- 1741 Morran, L. T., M. D. Parmenter, and P. C. Phillips, 2009 Muta- 1803
1742 tion load and rapid adaptation favour outcrossing over self- 1804
1743 fertilization. *Nature* **462**: 350–352. 1805
- 1744 MUKAI, T., 1967 *Synergistic interaction of spontaneous mutant poly-* 1806
1745 *genes controlling viability in Drosophila melanogaster*. *Genetics*. 1807
- 1746 Murray, R. L., J. L. Kozłowska, and A. D. Cutter, 2011 Heritable 1808
1747 determinants of male fertilization success in the nematode 1809
1748 *Caenorhabditis elegans*. *BMC evolutionary biology* **11**: 99. 1810
- 1749 Neher, R. A. and B. I. Shraiman, 2009 Competition between 1811
1750 recombination and epistasis can cause a transition from allele 1812
1751 to genotype selection. *Proceedings of the National Academy* 1813
1752 *of Sciences of the United States of America* **106**: 6866–6871. 1814
- 1753 Nigon, V., 1949 Les modalités de la reproduction et le deter- 1815
1754 minisme du sexe chez quelques nematodes libres. *Annales de* 1816
1755 *Sciences Naturelles - Zool. Biol. Anim.* **11**: 1–132. 1817
- 1756 Noble, L. M., A. S. Chang, D. McNelis, M. Kramer, M. Yen, 1818
1757 J. P. Nicodemus, D. D. Riccardi, P. Ammerman, M. Phillips, 1819
1758 T. Islam, and M. V. Rockman, 2015 Natural Variation in *plep-1* 1820
1759 Causes Male-Male Copulatory Behavior in *C. elegans*. *Current* 1821
1760 *biology* : **CB 25**: 2730–2737. 1822
- 1761 Paaby, A. B., A. G. White, D. D. Riccardi, K. C. Gunsalus, F. Piano, 1823
1762 and M. V. Rockman, 2015 Wild worm embryogenesis harbors 1824
1763 ubiquitous polygenic modifier variation. *eLife* **4**: 1061. 1825
- 1764 Pascual, L., N. Desplat, B. E. Huang, A. Desgroux, L. Bruguier, 1826
1765 J.-P. Bouchet, Q. H. Le, B. Chauchard, P. Verschave, and 1827
1766 M. Causse, 2015 Potential of a tomato MAGIC population 1828
1767 to decipher the genetic control of quantitative traits and detect 1829
1768 causal variants in the resequencing era. *Plant biotechnology* 1830
1769 *journal* **13**: 565–577. 1831
- 1770 Philip, V. M., G. Sokoloff, C. L. Ackert-Bicknell, M. Striz, 1832
1771 L. Branstetter, M. A. Beckmann, J. S. Spence, B. L. Jackson, 1833
1772 L. D. Galloway, P. Barker, A. M. Wymore, P. R. Hunsicker, 1834
1773 D. C. Durtschi, G. S. Shaw, S. Shinpock, K. F. Manly, D. R. 1835
1774 Miller, K. D. Donohue, C. T. Culiati, G. A. Churchill, W. R. Lar- 1836
1775 iviere, A. A. Palmer, B. F. O'Hara, B. H. Voy, and E. J. Chesler, 1837
1776 2011 Genetic analysis in the Collaborative Cross breeding 1838
1777 population. *Genome research* **21**: 1223–1238. 1839
- 1778 Phillips, N., M. Salomon, A. Custer, D. Ostrow, and C. F. 1840
1779 Baer, 2009 Spontaneous mutational and standing genetic 1841
1780 (co)variation at dinucleotide microsatellites in *Caenorhabditis* 1842
1781 *briggsae* and *Caenorhabditis elegans*. *Molecular biology and* 1843
1782 *evolution* **26**: 659–669. 1844
- 1783 Phillips, P. C., 2008 Epistasis - the essential role of gene interac- 1845
1784 tions in the structure and evolution of genetic systems. *Nature* 1846
1785 *Reviews Genetics* **9**: 855–867. 1847
- 1786 Phillips, P. C., S. P. Otto, and M. C. Whitlock, 2000 Beyond the 1848
1787 average. In *Epistasis and the Evolutionary Process*, edited by J. B. 1849
1788 Wolf, E. D. Brodie, and M. J. Wade, Oxford University Press. 1850
- Poelwijk, F. J., S. Tănase-Nicola, D. J. Kiviet, and S. J. Tans, 2011
Reciprocal sign epistasis is a necessary condition for multi-
peaked fitness landscapes. *Journal of theoretical biology* **272**:
141–144.
- Pouillet, N., A. Vielle, C. Gimond, S. Carvalho, H. Teotónio, and
C. Braendle, 2016 Complex heterochrony underlies the evolu-
tion of *Caenorhabditis elegans* hermaphrodite sex allocation **70**:
2357–2369.
- Pritchard, J. K., 2002 The allelic architecture of human disease
genes: common disease-common variant... or not? *Human*
molecular genetics **11**: 2417–2423.
- Reddy, K. C., E. C. Andersen, L. Kruglyak, and D. H. Kim,
2009 A polymorphism in *npr-1* is a behavioral determinant of
pathogen susceptibility in *C. elegans*. *Science (New York, N.Y.)*
323: 382–384.
- Robinson, G. K., 1991 That BLUP is a good thing: the estimation
of random effects. *Statistical science* .
- Rockman, M. V. and L. Kruglyak, 2008 Breeding designs for
recombinant inbred advanced intercross lines. *Genetics* **179**:
1069–1078.
- Rockman, M. V. and L. Kruglyak, 2009 Recombinational land-
scape and population genomics of *Caenorhabditis elegans*. *PLOS*
Genetics **5**: e1000419.
- Rockman, M. V., S. S. Skrovaneck, and L. Kruglyak, 2010 Selection
at linked sites shapes heritable phenotypic variation in *C.*
elegans. *Science (New York, N.Y.)* **330**: 372–376.
- Ruby, J. G., C. Jan, C. Player, M. J. Axtell, W. Lee, C. Nusbaum,
H. Ge, and D. P. Bartel, 2006 Large-scale sequencing reveals
21U-RNAs and additional microRNAs and endogenous siR-
NAs in *C. elegans*. *Cell* **127**: 1193–1207.
- Schoustra, S., S. Hwang, J. Krug, and J. A. G. M. de Visser, 2016
Diminishing-returns epistasis among random beneficial muta-
tions in a multicellular fungus. *Proc. R. Soc. B* **283**: 20161376.
- Seidel, H. S., M. Ailion, J. Li, A. van Oudenaarden, M. V. Rock-
man, and L. Kruglyak, 2011 A novel sperm-delivered toxin
causes late-stage embryo lethality and transmission ratio dis-
tortion in *C. elegans*. *PLoS biology* **9**: e1001115.
- Seidel, H. S., M. V. Rockman, and L. Kruglyak, 2008 Widespread
genetic incompatibility in *C. elegans* maintained by balancing
selection. *Science (New York, N.Y.)* **319**: 589–594.
- Seyfert, A. L., M. E. A. Cristescu, L. Frisse, S. Schaack, W. K.
Thomas, and M. Lynch, 2008 The Rate and Spectrum of Mi-
crosatellite Mutation in *Caenorhabditis elegans* and *Daphnia*
pulex. *Genetics* **178**: 2113–2121.
- Shao, H., L. C. Burrage, D. S. Sinasac, A. E. Hill, S. R. Ernest,
W. O'Brien, H.-W. Courtland, K. J. Jepsen, A. Kirby, E. J. Kul-
bokas, M. J. Daly, K. W. Broman, E. S. Lander, and J. H.
Nadeau, 2008 Genetic architecture of complex traits: large
phenotypic effects and pervasive epistasis. **105**: 19910–19914.
- Shen, X., M. Alam, L. Ronnegard, and M. X. Shen, 2014 Package
'hglm' .
- Simon, M., O. Loudet, S. Durand, A. Bérard, D. Brunel, F.-X. Sen-
nesal, M. Durand-Tardif, G. Pelletier, and C. Camilleri, 2008
Quantitative trait loci mapping in five new large recombinant
inbred line populations of *Arabidopsis thaliana* genotyped with
consensus single-nucleotide polymorphism markers. *Genetics*
178: 2253–2264.
- Sokal, R. R. and F. J. Rohlf, 1995 *Biometry: the principles and*
practice of statistics in biological sciences. WH Free Company.
- Speed, D. and D. J. Balding, 2015 Relatedness in the post-
genomic era: is it still useful? *Nature Reviews Genetics* **16**:
33–44.

LITERATURE CITED

LITERATURE CITED

- Speed, D., N. Cai, T. U. Consortium, M. Johnson, S. Nejentsev, and D. Balding, 2016 Re-evaluation of SNP heritability in complex human traits. *bioRxiv* p. 074310.
- Speed, D., G. Hemani, M. R. Johnson, and D. J. Balding, 2012 Improved heritability estimation from genome-wide SNPs. *American journal of human genetics* **91**: 1011–1021.
- Sterken, M. G., L. B. Snoek, J. E. Kammenga, and E. C. Andersen, 2015 The laboratory domestication of *Caenorhabditis elegans*. *Trends in genetics : TIG* **31**: 224–231.
- Stewart, A. D. and P. C. Phillips, 2002 Selection and maintenance of androdioecy in *Caenorhabditis elegans*. *Genetics* **160**: 975–982.
- Stiernagle, T., 2006 Maintenance of *C. elegans*. *WormBook : the online review of C. elegans biology* pp. 1–11.
- Swierczek, N. A., A. C. Giles, C. H. Rankin, and R. A. Kerr, 2011 High-throughput behavioral analysis in *C. elegans*. *Nature methods* **8**: 592–598.
- Teotónio, H., S. Carvalho, D. Manoel, M. Roque, and I. M. Chelo, 2012 Evolution of outcrossing in experimental populations of *Caenorhabditis elegans*. *PloS one* **7**: e35811.
- Teotónio, H., S. Estes, P. C. Phillips, and C. F. Baer, 2017 Evolution experiments with *Caenorhabditis* nematodes. *Genetics* .
- Teotónio, H., D. Manoel, and P. C. Phillips, 2006 Genetic Variation for Outcrossing among *Caenorhabditis elegans* Isolates **60**: 1300–1305.
- Theologidis, I., I. M. Chelo, C. Goy, and H. Teotónio, 2014 Reproductive assurance drives transitions to self-fertilization in experimental *Caenorhabditis elegans*. *BMC biology* **12**: 93.
- Thepot, S., G. Restoux, I. Goldringer, F. Hospital, D. Gouache, I. Mackay, and J. Enjalbert, 2015 Efficient Tracking Selection in a Multiparental Population: The Case of Earliness in Wheat. *Genetics* **199**: 609–623.
- Thompson, O. A., L. B. Snoek, H. Nijveen, M. G. Sterken, R. J. M. Volkers, R. Brenchley, A. Van't Hof, R. P. J. Bevers, A. R. Cossins, I. Yanai, A. Hajnal, T. Schmid, J. D. Perkins, D. Spencer, L. Kruglyak, E. C. Andersen, D. G. Moerman, L. W. Hillier, J. E. Kammenga, and R. H. Waterston, 2015 Remarkably Divergent Regions Punctuate the Genome Assembly of the *Caenorhabditis elegans* Hawaiian Strain CB4856. *Genetics* **200**: 975–989.
- Tyler, A. L., L. R. Donahue, G. A. Churchill, and G. W. Carter, 2016 Weak Epistasis Generally Stabilizes Phenotypes in a Mouse Intercross. *PLOS Genetics* **12**: e1005805.
- Valdar, W., L. C. Solberg, D. Gauguier, S. Burnett, P. Klenerman, W. O. Cookson, M. S. Taylor, J. N. P. Rawlins, R. Mott, and J. Flint, 2006 Genome-wide genetic association of complex traits in heterogeneous stock mice. *Nature Genetics* **38**: 879–887.
- Vanhaeren, H., N. Gonzalez, F. Coppens, L. De Milde, T. Van Daele, M. Vermeersch, N. B. Eloy, V. Storme, and D. Inzé, 2014 Combining growth-promoting genes leads to positive epistasis in *Arabidopsis thaliana*. *eLife* **3**: e02252.
- VanRaden, P. M., 2008 Efficient methods to compute genomic predictions. *Journal of dairy science* **91**: 4414–4423.
- Visscher, P. M., G. Hemani, A. A. E. Vinkhuyzen, G.-B. Chen, S. H. Lee, N. R. Wray, M. E. Goddard, and J. Yang, 2014 Statistical power to detect genetic (co)variance of complex traits using SNP data in unrelated samples. *PLOS Genetics* **10**: e1004269.
- Visscher, P. M., B. McEVOY, and J. Yang, 2010 From Galton to GWAS: quantitative genetics of human height. *Genetics Research* **92**: 371–379.
- Weigel, D., 2012 Natural variation in Arabidopsis: from molecular genetics to ecological genomics. *Plant physiology* **158**: 2–22.
- Weinreich, D. M., Y. Lan, C. S. Wylie, and R. B. Heckendorn, 2013 Should evolutionary geneticists worry about higher-order epistasis? *Current opinion in genetics & development* **23**: 700–707.
- Weinreich, D. M., R. A. Watson, and L. Chao, 2005 Perspective: Sign epistasis and genetic constraint on evolutionary trajectories. *Evolution* **59**: 1165–1174.
- Whitlock, M. C. and D. Bourguet, 2000 FACTORS AFFECTING THE GENETIC LOAD IN DROSOPHILA: SYNERGISTIC EPISTASIS AND CORRELATIONS AMONG FITNESS COMPONENTS. *Evolution* **54**: 1654.
- Whitlock, M. C., P. C. Phillips, F. B. G. Moore, and S. J. Tonsor, 1995 Multiple Fitness Peaks and Epistasis. *Annual Review of Ecology and Systematics* **26**: 601–629.
- Wolf, J. B., E. D. Brodie, and M. J. Wade, editors, 2000 *Epistasis and the Evolutionary Process*. Oxford University Press.
- Wood, A. R., T. Esko, J. Yang, S. Vedantam, T. H. Pers, S. Gustafsson, A. Y. Chu, K. Estrada, J. Luan, Z. Kutalik, N. Amin, M. L. Buchkovich, D. C. Croteau-Chonka, F. R. Day, Y. Duan, T. Fall, R. Fehrmann, T. Ferreira, A. U. Jackson, J. Karjalainen, K. S. Lo, A. E. Locke, R. Mägi, E. Mihailov, E. Porcu, J. C. Randall, A. Scherag, A. A. E. Vinkhuyzen, H.-J. Westra, T. W. Winkler, T. Workalemahu, J. H. Zhao, D. Absher, E. Albrecht, D. Anderson, J. Baron, M. Beekman, A. Demirkan, G. B. Ehret, B. Feenstra, M. F. Feitosa, K. Fischer, R. M. Fraser, A. Goel, J. Gong, A. E. Justice, S. Kanoni, M. E. Kleber, K. Kristiansson, U. Lim, V. Lotay, J. C. Lui, M. Mangino, I. Matteo Leach, C. Medina-Gomez, M. A. Nalls, D. R. Nyholt, C. D. Palmer, D. Pasko, S. Pechlivanis, I. Prokopenko, J. S. Ried, S. Ripke, D. Shungin, A. Stancáková, R. J. Strawbridge, Y. J. Sung, T. Tanaka, A. Teumer, S. Trompet, S. W. van der Laan, J. van Setten, J. V. van Vliet-Ostaptchouk, Z. Wang, L. Yengo, W. Zhang, U. Afzal, J. Arnlöv, G. M. Arscott, S. Bandinelli, A. Barrett, C. Bellis, A. J. Bennett, C. Berne, M. Blüher, J. L. Bolton, Y. Böttcher, H. A. Boyd, M. Bruinenberg, B. M. Buckley, S. Buyske, I. H. Caspersen, P. S. Chines, R. Clarke, S. Claudi-Boehm, M. Cooper, E. W. Daw, P. A. De Jong, J. Deelen, G. Delgado, J. C. Denny, R. Dhonukshe-Rutten, M. Dimitriou, A. S. F. Doney, M. Dörr, N. Eklund, E. Eury, L. Folkersen, M. E. Garcia, F. Geller, V. Giedraitis, A. S. Go, H. Grallert, T. B. Grammer, J. Gräßler, H. Grönberg, L. C. P. G. M. de Groot, C. J. Groves, J. Haessler, P. Hall, T. Haller, G. Hallmans, A. Hannemann, C. A. Hartman, M. Hassinen, C. Hayward, N. L. Heard-Costa, Q. Helmer, G. Hemani, A. K. Henders, H. L. Hillege, M. A. Hlatky, W. Hoffmann, P. Hoffmann, O. Holmen, J. J. Houwing-Duistermaat, T. Illig, A. Isaacs, A. L. James, J. Jeff, B. Johansen, Å. Johansson, J. Jolley, T. Juliusdottir, J. Juntila, A. N. Kho, L. Kinnunen, N. Klopp, T. Kocher, W. Kratzer, P. Lichtner, L. Lind, J. Lindström, S. Lobbens, M. Lorentzon, Y. Lu, V. Lyssenko, P. K. E. Magnusson, A. Mahajan, M. Maillard, W. L. McArdle, C. A. McKenzie, S. McLachlan, P. J. McLaren, C. Menni, S. Merger, L. Milani, A. Moayyeri, K. L. Monda, M. A. Morken, G. Müller, M. Müller-Nurasyid, A. W. Musk, N. Narisu, M. Nauck, I. M. Nolte, M. M. Nöthen, L. Oozageer, S. Pils, N. W. Rayner, F. Renström, N. R. Robertson, L. M. Rose, R. Roussel, S. Sanna, H. Scharnagl, S. Scholtens, F. R. Schumacher, H. Schunkert, R. A. Scott, J. Sehmi, T. Seufferlein, J. Shi, K. Silventoinen, J. H. Smit, A. V. Smith, J. Smolonska, A. V. Stanton, K. Stirrups, D. J. Stott, H. M. Stringham, J. Sund-

- 1975 ström, M. A. Swertz, A.-C. Syvänen, B. O. Tayo, G. Thorleifsson,
1976 J. P. Tyrer, S. van Dijk, N. M. van Schoor, N. van der Velde,
1977 D. van Heemst, F. V. A. van Oort, S. H. Vermeulen, N. Ver-
1978 weij, J. M. Vonk, L. L. Waite, M. Waldenberger, R. Wennauer,
1979 L. R. Wilkens, C. Willenborg, T. Wilsgaard, M. K. Wojczynski,
1980 A. Wong, A. F. Wright, and Q. Zhang, 2014 Defining the role of
1981 common variation in the genomic and biological architecture
1982 of adult human height. *Nature Genetics* **46**: 1173–1186.
- 1983 Wray, G. A., 2007 The evolutionary significance of cis-regulatory
1984 mutations. *Nature Reviews Genetics* **8**: 206–216.
- 1985 Wright, S., 1932 The roles of mutation, inbreeding, crossbreeding,
1986 and selection in evolution.
- 1987 Yang, J., B. Benyamin, B. P. McEvoy, S. Gordon, A. K. Henders,
1988 D. R. Nyholt, P. A. Madden, A. C. Heath, N. G. Martin, G. W.
1989 Montgomery, M. E. Goddard, and P. M. Visscher, 2010 Com-
1990 mon SNPs explain a large proportion of the heritability for
1991 human height. *Nature Genetics* **42**: 565–569.
- 1992 Yang, J., T. A. Manolio, L. R. Pasquale, E. Boerwinkle, N. Caporaso,
1993 J. M. Cunningham, M. de Andrade, B. Feenstra, E. Feingold,
1994 M. G. Hayes, W. G. Hill, M. T. Landi, A. Alonso, G. Lettre,
1995 P. Lin, H. Ling, W. Lowe, R. A. Mathias, M. Melbye, E. Pugh,
1996 M. C. Cornelis, B. S. Weir, M. E. Goddard, and P. M. Visscher,
1997 2011 Genome partitioning of genetic variation for complex
1998 traits using common SNPs. *Nature Genetics* **43**: 519–525.
- 1999 Zheng, C., M. P. Boer, and F. A. van Eeuwijk, 2015 Reconstruc-
2000 tion of Genome Ancestry Blocks in Multiparental Populations.
2001 *Genetics* **200**: 1073–1087.
- 2002 Zheng, C., M. P. Boer, and F. A. van Eeuwijk, 2014 A general mod-
2003 eling framework for genome ancestral origins in multiparental
2004 populations. *Genetics* **198**: 87–101.
- 2005 Zwarts, L., M. M. Magwire, M. A. Carbone, M. Versteven,
2006 L. Herteleer, R. R. H. Anholt, P. Callaerts, and T. F. C. Mackay,
2007 2011 Complex genetic architecture of *Drosophila* aggressive
2008 behavior. *Proceedings of the National Academy of Sciences of
2009 the United States of America* **108**: 17070–17075.